

Geochemistry and Petrogenesis of Late Neoproterozoic Dokhan Volcanics at Wadi Abu Hamra area, Central Eastern Desert, Egypt

Hatem M. El-Desoky

Geology Department, Faculty of Science, Al-Azhar University
hatem_eldesoky2002@yahoo.com

Abstract: The present work deals with geology, petrography, geochemistry, petrogenesis and tectonic environment of Dokhan volcanics at Wadi Abu Hamra area. The studied Dokhan volcanics have composition of rhyolites, spherulitic rhyolites, rhyodacites, quartz dacites, bedded dacitic tuffs and subordinate andesitic tuffs. Rhyolites are usually found as large outcrops in the western part of the Gabal Abu Hamra area. Spherulitic rhyolites contain veinlets of quartz and minor outcrops occur at the beginning of Wadi Abu Hamra. Dacites are found as microcrystalline hard rocks of brownish grey in color and massive structure. Andesitic tuffs are characterized by dark grey, very fine-grained to glassy and sheared. Petrochemical characteristics and trace element distribution indicate that the Dokhan volcanics are calc-alkaline in nature with a rather tholeiitic affinity. The Dokhan volcanics represent a well developed active continental margin or island arc with a thick continental crust. The behavior of many elements supports mantle as well as crustal affinities. Association of both mantle and crust suggests deep source, probably the mantle, and differentiation of the magma as it ascended into the crust with which it interacted. The initiation and termination of the eruption in divergent settings indicate that the magmatic activities were generated from a common source. The final emplacement of the Dokhan volcanics in a continental setting is suggestive of a prolonged divergent activity initiated at great depth. The magma traced and utilized the rift until the last batch completely solidified as rhyolites, rhyodacites and tuffs on the continent.

[Hatem M. El-Desoky. **Geochemistry and Petrogenesis of Late Neoproterozoic Dokhan Volcanics at Wadi Abu Hamra area, Central Eastern Desert, Egypt** *J Am Sci* 2013;9(5):212-235]. (ISSN: 1545-1003).

<http://www.jofamericanscience.org>. 28

Key words: Dokhan volcanics, geochemistry, Neoproterozoic, petrogenesis, petrography, geotectonic and Egypt.

Introduction

The chief aiming of the present paper is elucidate geology, petrography, geochemistry, petrogenesis and tectonic environment of Dokhan volcanics at Wadi Abu Hamra area. That lies between latitudes 26° 17' 06" and 26° 19' 07" N and Longitudes 34° 05' 05" and 34° 07' 09" E, covering about 35 kilometers square. It is located north Wadi Hamrawein of metagabbro-diorite complex and lies 25 km northwest Quseir City. The examined area is accessible through the Red Sea costal asphaltic road.

The area consists largely of island arc system (Intermediate metavolcanics) and extruded by Dokhan volcanics. The Dokhan volcanics are most abundantly occurring in the Northern part of the Eastern Desert of Egypt and related to Late Proterozoic products of the Pan-African volcanism in the Nubian Shield. The volcanic and volcanoclastic rocks covering vast areas in the Eastern Desert of Egypt are represented by metavolcanics and Dokhan volcanics. These Dokhan volcanic rocks constitute a group of calc-alkaline extrusion and well developed in various parts of the Eastern Desert.

The geotectonic interpretation of the Dokhan volcanics has been highly debated with models centered on three main settings:-

(1) Anorogenic setting: intra-continental rift model

similar to the Oslo rift system in Norway (**Stern and Gottfried, 1986**).

(2) Orogenic setting: active continental margin (**El Gaby et al., 1989 and El Sheshtawi et al., 1997**).

(3) Transitional setting: between compressional and extensional settings (**Mohamed et al., 2000**).

Garson and Shalaby (1976) have proposed a plate tectonic setting for Red Sea orogenies. According to these authors, the Dokhan volcanics were apparently emplaced on the active continental margin (Andean type movement) above the steeply-dipping end phase of the Quseir-Berenice Benioff zone. **Ries et al. (1983)** stated that the Dokhan volcanics possibly originated by crystallization differentiation from a normal tholeiitic basaltic magma or derivative of andesitic magma intermediate in composition.

Hassan (1987) mentioned that the Dokhan volcanics are continental alkaline volcanics poor in lime. **Ragab (1987)** studied the Dokhan volcanics of the Northern Eastern Desert and reported that, the Dokhan volcanics belong to the low-K calc-alkaline subseries which matches with the Cascade Range. Their geotectonic environment is characterized by ensimatic mature island arcs, in which the low-K calc-alkaline magmatic arcs were preceded by immature island arcs.

The geochemical bimodality of the Dokhan volcanics and their enrichment in K, Nb, Zr and other incompatible elements, criteria which appear to be earmarks of two specific tectonic settings, viz. subduction-related and within plate settings (**Pearce, 1983**).

Akaad and Abu El-Ela (2002) mentioned that the Dokhan volcanics possess the following field relationships:-

- Occur unconformably over arc metasediments, either as large exposures or else as small outliers oriented NNW.
- The large Dokhan outcrops are variably covered with Iгла Formation in distinct unconformity, showing the normal lithostratigraphic setup.
- Constitute, wholly or partly, downfaulted blocks, alone or together with the overriding Iгла Formation. The downfaulting may be against arc assemblage, Iгла Formation or Younger Granites.
- Intruded by Post-Hammamat Felsites, particularly in the corner of the study region, N and NW of W. Saqia and Wadi Abu Shigeili. The Dokhan volcanics are also intruded by various Younger Granites, such as the Gabal Um Zarabit granodiorite-monzonite and others.

Geologic setting

Wadi Abu Hamra Dokhan volcanics form moderate to relatively high mountains covering more than 30 km² of the mapped area (Fig.1). They are sheeted and dissected often by vertical and horizontal joints in NW-SE direction. At the studied area, the most common types among the Dokhan volcanics are rhyolites, spherulitic rhyolites, dacites, less frequent rhyodacites and dacites intercalations and andesitic tuff deposits (consolidated ash) are commonly interbedded with lava flows successions.

The transition between the rhyolite core and spherulitic rhyolite peripheries has been detected. Alternation of felsitic rhyolite and spherulitic rhyolite layers of different thickness is typical of the Gabal Abu Hamra, whereas rhyodacites enclosed in dacite matrix occur in the peripheries of the Gabal Abu Hamra.

Rhyolites are usually found as large outcrops in the western part of the studied area. Felsite rocks are fairly homogeneous with apparent variations. These rocks show gradational contacts with the dacite volcanics (Fig.2a). The pyroclastic rocks in the studied area are mainly of basic, intermediate or acidic composition and represented mainly by volcanic tuffs. Acidic volcanic rocks cover the western side of Wadi Abu Hamra area usually forming horizontal sheets and sills.

Spherulitic rhyolites contain veinlets of quartz and minor outcrops occur at the beginning of Wadi Abu Hamra (Fig.2b). This volcanic is characterized

by light grey, buff and reddish colors and the mineral assemblages are essentially represented by quartz, alkali feldspar and plagioclase. Spherulitic felsite is typically composed of alkali feldspar and quartz with minor iron oxides. Subsequent to emplacement, the quenched glass gradually hydrates to grey rhyolite. Although the spherulitic rhyolites are sometimes jointed and faulted, there is no evidence for folding.

Dacites and rhyodacites often occur in lesser amount than rhyolites and are found as microcrystalline hard rocks of brownish grey, greyish green color and massive structure. Bedded dacitic tuffs are characterized by pale olive grey laminated and fine-grained to glassy (Fig.2c). The dacitic rocks are observed as relatively small spots and sheets associated with the spherulitic rhyolites and rhyolitic rocks without sharp contact.

Andesitic tuffs (consolidated ash) are characterized by dark grey to greenish grey color, very fine-grained to glassy and sheared (Fig.2d). They are usually composed of badly sorted, angular to subangular fragments cemented together by andesitic matrix and found blended with the previously mentioned volcanic rocks.

Petrography

The Dokhan volcanics of the study area cover a limited range in composition. They include essentially rhyolites, spherulitic rhyolites, rhyodacites and dacites with subordinate bedded dacitic tuffs and andesitic tuffs.

Rhyolites

Rhyolite shows mainly porphyritic and glomeroporphyritic textures (Fig.3a). It is formed essentially by phenocrysts of quartz, plagioclase and potash feldspars (orthoclase) embedded in a fine-grained groundmass. Chlorite, sericite and epidote are secondary mineral, whereas zircon and iron oxides are accessories.

Quartz forms large anhedral to subhedral phenocrysts reaching up to 0.5mm in width and 0.9mm in length as well as small interstitial grains of fine aggregates in the groundmass (Fig.3b). Quartz also occurs as thin streaks in the groundmass or as recrystallized fine-grained quartz in microveinlets (Fig.3c). They show undulose extinction and contain some inclusions of iron oxides. **Plagioclase** forms subhedral, elongated crystals up to 0.2mm wide and 0.5mm long with distinct lamellar twinning (Fig.3d). They are partially altered to epidote and saussurite. The crystals are corroded by quartz, iron oxides and potash feldspar. **Orthoclase** forms subhedral crystals associating plagioclase and quartz, partly altered to sericite and clay minerals (Fig.3e). The crystals show simple twinning and the products of alteration are mainly sericite. **Sericite** is the main secondary mineral and occurs as colorless interstitial flakes

between quartz and feldspar or enclosed within them (Fig.3f). **Chlorite** is pale green and it occurs as fine flakes being concentrated in the groundmass. **Epidote** granules represent the main alteration products of plagioclase crystals. **Zircon** usually

occurs as minute crystals of short prismatic habit and often found as inclusions with high relief. **Iron oxide** forms irregularly scattered grains and inclusions in the feldspars and quartz (Fig.3f).

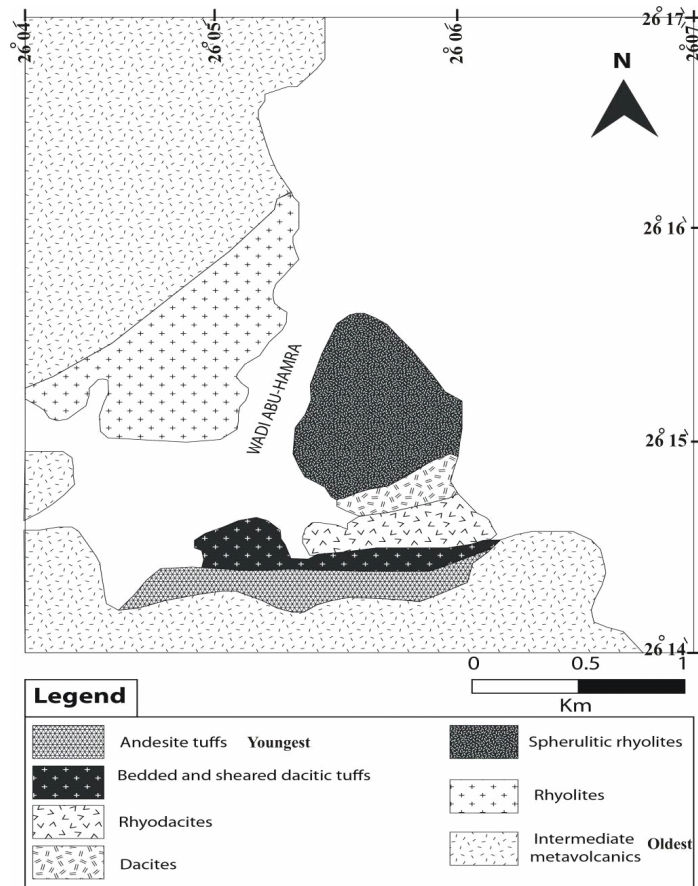
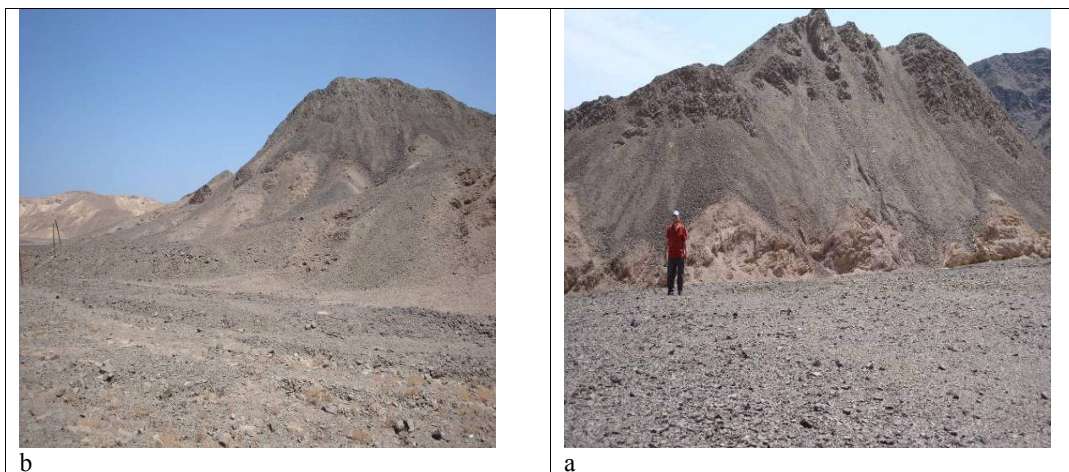


Fig.1: Geological map of Abu Hamra area (Modified after Akaad and Abu El-Ela, 2002).



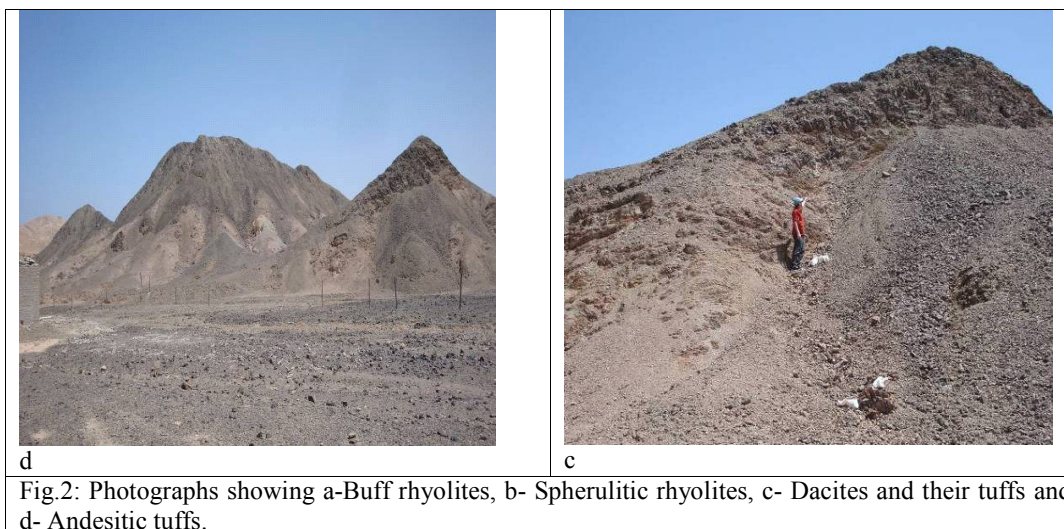


Fig.2: Photographs showing a- Buff rhyolites, b- Spherulitic rhyolites, c- Dacites and their tuffs and d- Andesitic tuffs.

Spherulitic rhyolites

Spherulitic rhyolites are composed mainly of phenocryst of quartz, plagioclase and orthoclase. Occasionally some scattered flakes of biotite and sericite are present. Chlorite and epidote are present as secondary minerals. The rock displays spherulitic texture as it contains spheres of fibrous orthoclase and quartz crystals radiating from a common center (Fig.4a). Spherulitic and porphyritic textures were recognized in the studied spherulitic rhyolites.

Quartz occurs as subhedral and anhedral phenocryst up to 0.5mm across, that are scattered in fine-grained groundmass and also found as anhedral aggregates interstitial to the groundmass. It is sometimes slightly elongated and exhibits mild to moderate deformation as indicated by the undulose extinction and sutured borders (Fig.4b). **Plagioclase** occurs as tabular subhedral crystals of albite ranging from 2.9 to 3.6 mm in length and from 2.4 to 3.0 mm in width. They show well-developed lamellar twinning. Small sericite flakes are found along the twinning planes (Fig.4c). **Orthoclase** occurs as subhedral crystals up to 3.1 mm in length and 2.2 mm in width. They are partly to totally altered to kaolin and sericite and it is sometimes show well-developed simple twinning (Fig.4d). **Biotite** occurs as brownish and pale brownish anhedral pleochroic flakes associated with the sericite crystals. Some flakes are strained and twisted; they are partly altered to chlorite (Fig.4e). **Sericite** commonly form minute scattered crystals up to 0.04 mm across (Fig.4f). **Chlorite** occurs as pale green flakes subhedral crystals and as irregular patches up to 0.6 mm across (Fig.4e). It may be formed after pyroxene indicated by the presence of relics of the later within chlorite. **Epidote** forms yellowish green aggregates, anhedral

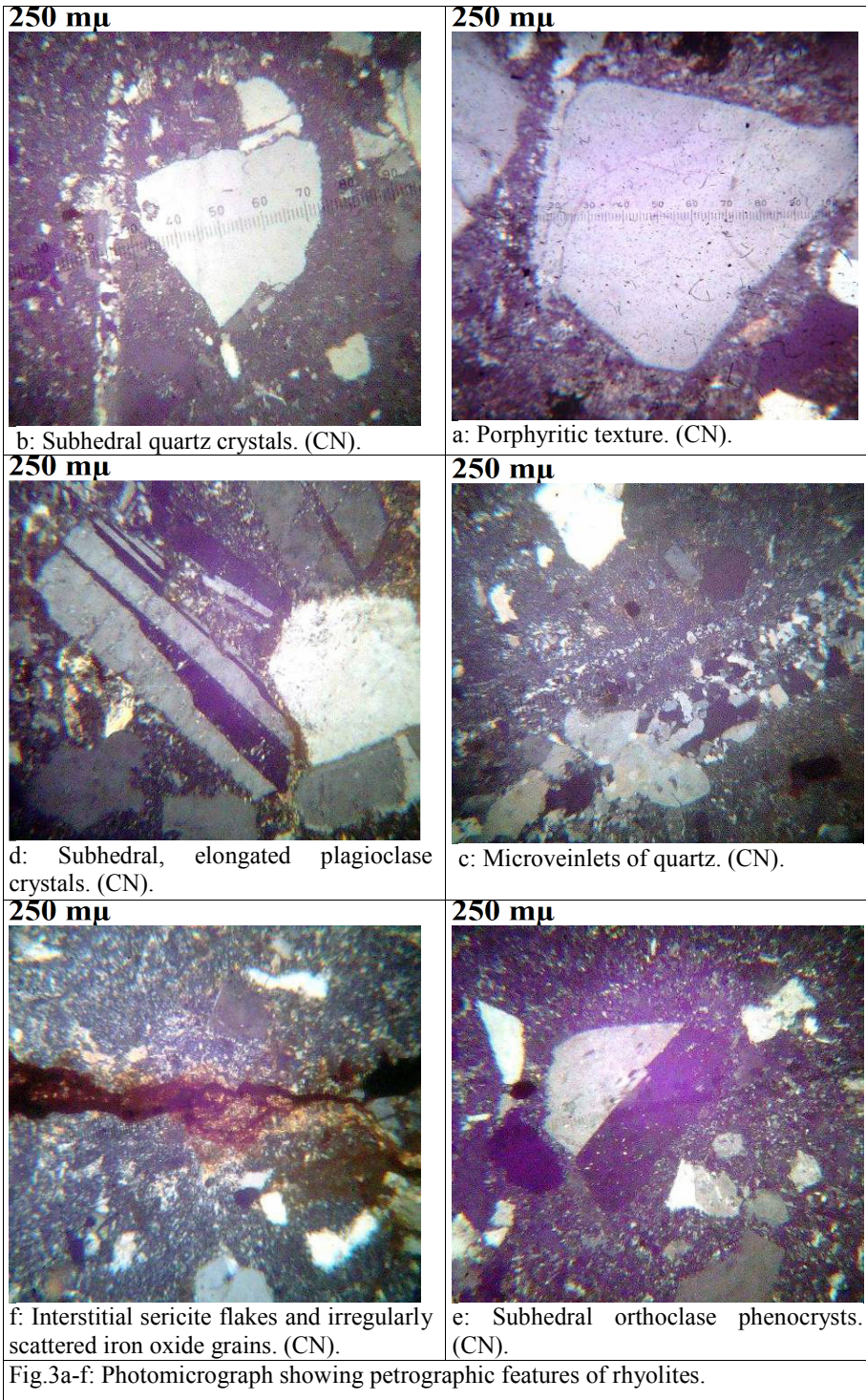
crystals associated with and sometimes replacing plagioclase crystals. It is accompanied with minor zoisite. **Zircon** occurs as minute inclusions in the other minerals (quartz and orthoclase). **Iron oxide** grains are irregularly scattered in the rock and also occur as inclusions in the feldspar and quartz (Fig.4c).

Rhyodacites

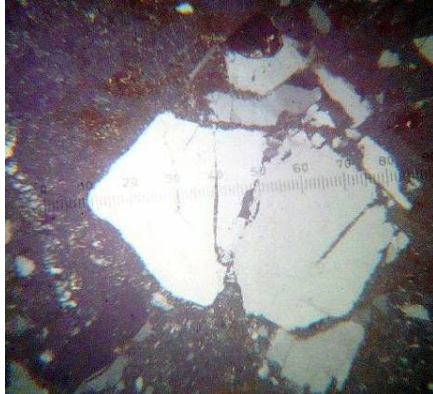
They show pinkish to pinkish grey color and porphyritic texture (Fig.5a). They consist of microphenocrysts of quartz, plagioclase, orthoclase with some sericite and iron oxides. The fine-grained groundmass consists of quartz aggregates, which fill some of microveinlets and amygdales in the groundmass.

Quartz is the predominant mineral and it is varying in size and form. It occurs as porphyritic crystals that have corroded margins and anhedral crystals filling the interstitials of the mineral constituents (Fig.5b). Occasionally, they show undulose extinction. **Plagioclase** occurs as coarse-grained subhedral crystals with anorthite content varying from An_{13} to An_{23} and sometimes, they are altered to saussurite (Fig.5a). **Orthoclase** occurs as subhedral crystals up to 0.7mm in length and 0.4mm in width. They are embedded in fine-grained matrix and partly altered to sericite and kaolin. Also, they have well developed simple twinning (Fig.5c).

Sericite is represented by fine flaky crystals encountered in the groundmass and occurs as alteration products of orthoclase (Fig.5c). **Iron oxide** forms brown irregular particles dispersed in the interstitial spaces between the other constituents and also represented as shapeless granules, 0.1 mm across.

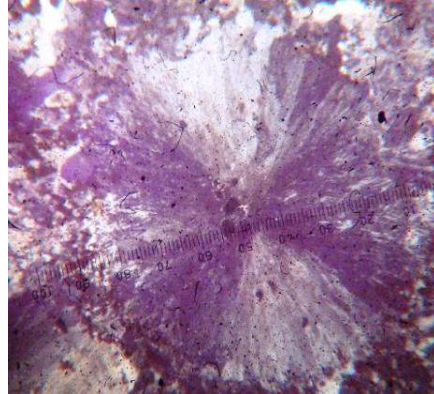


250 μ m



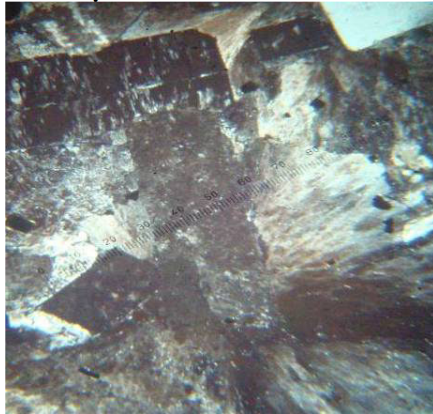
b: Subhedral, sutured borders of quartz crystals. (CN).

250 μ m



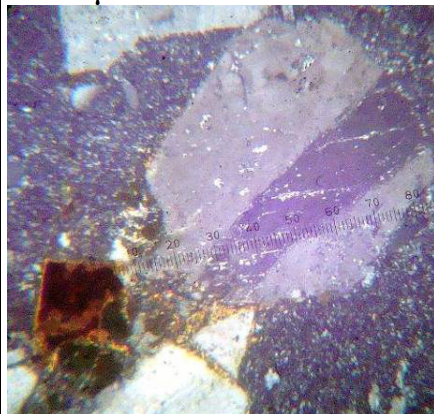
a: Spherulitic texture. (CN).

250 μ m



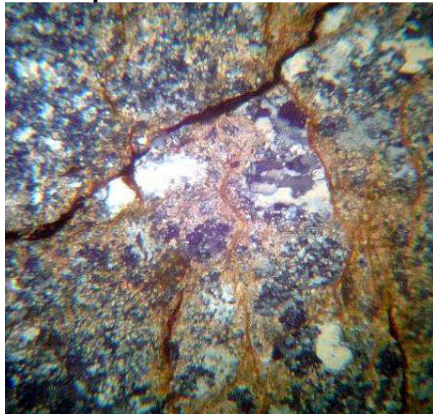
d: Fibrous orthoclase and quartz crystals radiating. (CN).

250 μ m



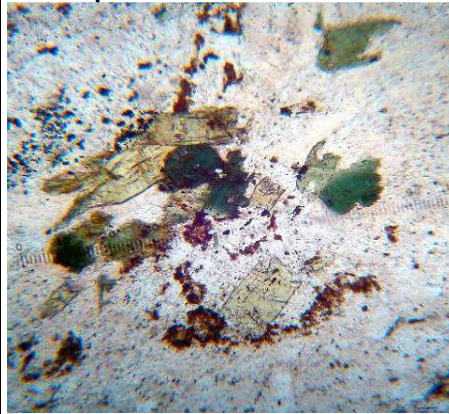
c: Carlsbad twinning in subhedral plagioclase crystals and iron oxides. (CN).

250 μ m



f: Minute scattered sericite crystals. (CN).

250 μ m



e: Biotite partly altered to chlorite. (PPL).

Fig.4a-f: Photomicrograph showing petrographic features of spherulitic rhyolites.

Dacites

These rocks consist essentially of plagioclase phenocrysts, orthoclase, hornblende and quartz set in fine-grained groundmass of quartz, chlorite, biotite and iron oxides. Chlorite and sericite are the main secondary minerals, while zircon, biotite and iron oxides are the main accessories.

Plagioclase is represented by subhedral crystals up to 0.4mm in width and 0.8mm in length with anorthite content ranging from An₁₃ to An₂₁. They show porphyritic texture and Carlsbad-lamellar twinning (Fig.5d). They are altered to saussurite and have corroded margins due to replacement by the finer tuffaceous matrix. **Orthoclase** forms subhedral crystals associating plagioclase; they are partly altered to clay minerals and sericite (Fig.5e). **Hornblende** occurs as subhedral microphenocrysts exhibiting brown color and baveno twinning, strongly pleochroic and two sets of cleavage characterizing the amphibole minerals (Fig.5f). Also, it forms fine aggregates and minute crystals in the groundmass. **Quartz** is represented by anhedral and subhedral crystals up to 0.5mm across that are scattered in fine-grained groundmass (Fig.5f). It commonly shows wavy and undulose extinction. Quartz is filling some of amygdales in the groundmass. **Sericite** occurs as fine flakes, 0.2 mm long as well as colorless interstitial flakes between quartz, plagioclase and in the groundmass (Fig.5e).

Bedded and sheared dacitic tuffs

Laminated lapilli dacitic tuffs is of very limited distribution and is composed essentially of microphenocrysts of rounded crystals of quartz together with plagioclase, hornblende and tremolite set in cryptocrystalline to glassy groundmass of biotite, chlorite and hematite (Fig.6a).

Quartz occurs as anhedral interstitial fine-grained and as rounded and subrounded grains up to 0.7 mm across and aggregates (Fig.6b). **Plagioclase** is found in minor amounts as untwinned subhedral crystals and is usually altered to saussurite. **Hornblende** occurs as subhedral microphenocrysts exhibiting pale green color, fine disseminated grains and irregular short minute prismatic crystals. Also, it forms fine aggregates and minute crystals in the groundmass (Fig.6c). **Tremolite** occurs as colorless subhedral crystals of short and long prismatic habit, 1.9 mm in length and 0.4 mm in width. Two directions of cleavage at angles of 56°, weak pleochroism and included crystal of quartz forming granular texture (Fig.6d).

Andesitic tuffs

Cryptocrystalline texture is common in tuffs

(consolidated ash), as in the matrix of this rock. The matrix encloses fragments of quartz, calcite, zircon and iron oxides (hematite) crystals (Fig.6e). The fragmented rock consists of crystals of quartz, alkali feldspar and plagioclase of various size and shapes, pieces of glassy rhyolite and pieces of fine-grained banded ash matrix are found.

Fine lithic-crystal tuffs are composed of angular to subangular crystal ashed which are represented mainly quartz together with subordinate plagioclase and chlorite; and lithic ashes which are represented by rhyolite together with subordinate felsite, dacite and glassy materials, all set in a microcrystalline tuffaceous matrix (Fig.6e).

Tuffaceous matrix is composed microcrystalline volcanic dust of quartz and subordinate plagioclase together with abundant chlorite flakes, iron oxide granules and carbonate patches (Fig.6f). These rocks are characterized by the presence of many microveinlets which is distributed in different directions and filled with quartz, hematite and calcite (Fig.6f).

Geochemistry

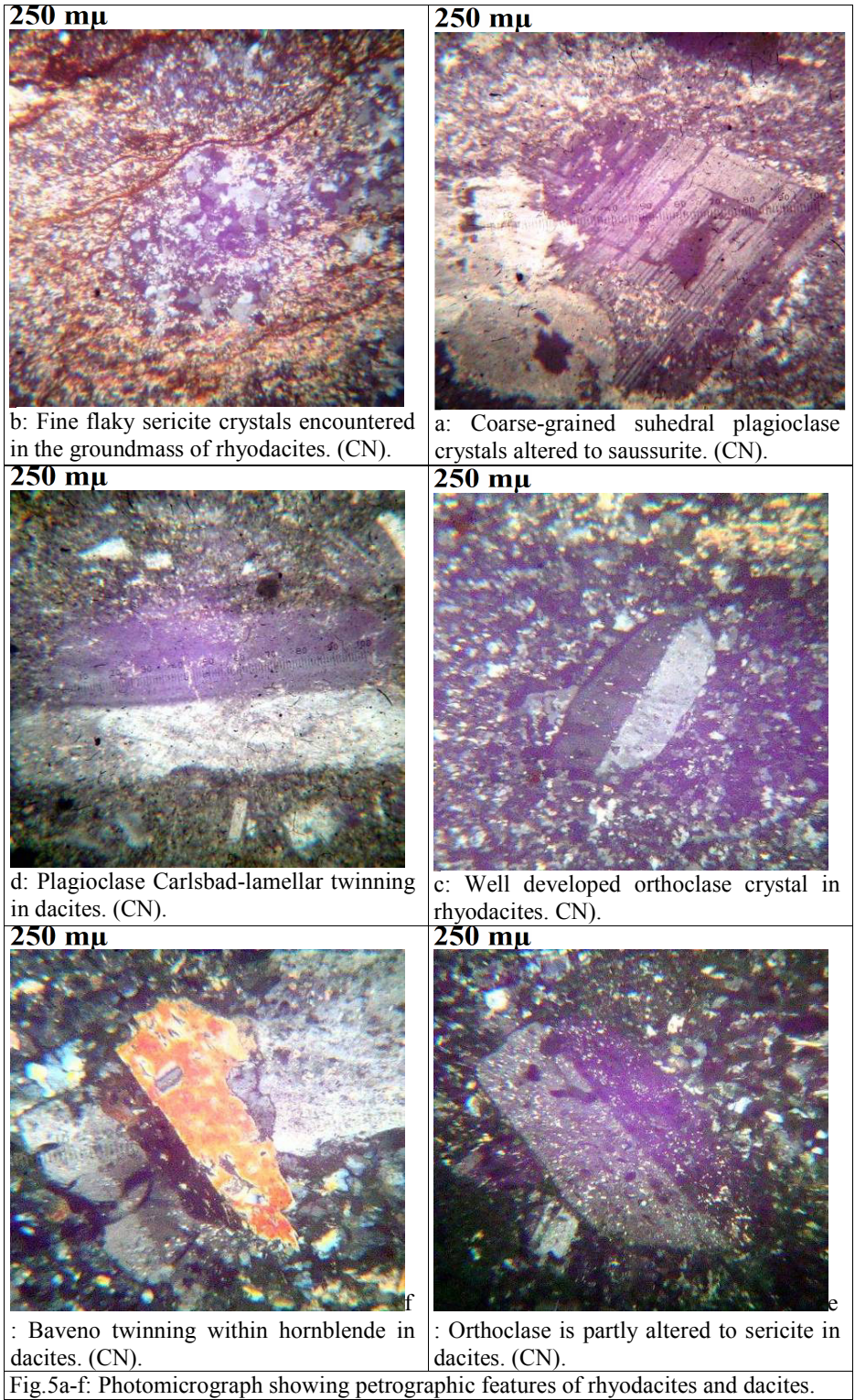
Using ICP technique, twenty six samples were analyzed for determination of major oxides and trace elements at the Central Laboratories of Nuclear Materials Authority (NMA). Bulk chemical analyses of samples from these volcanic rocks are given in **Table 1** (rhyolites and spherulitic rhyolites), **Table 2** (rhyodacites and dacites) and **Table 3** (bedded dacitic tuffs and andesitic tuffs). All analyzed and calculated data are used to clarify the chemical classification, magma type, petrogenesis and tectonic settings.

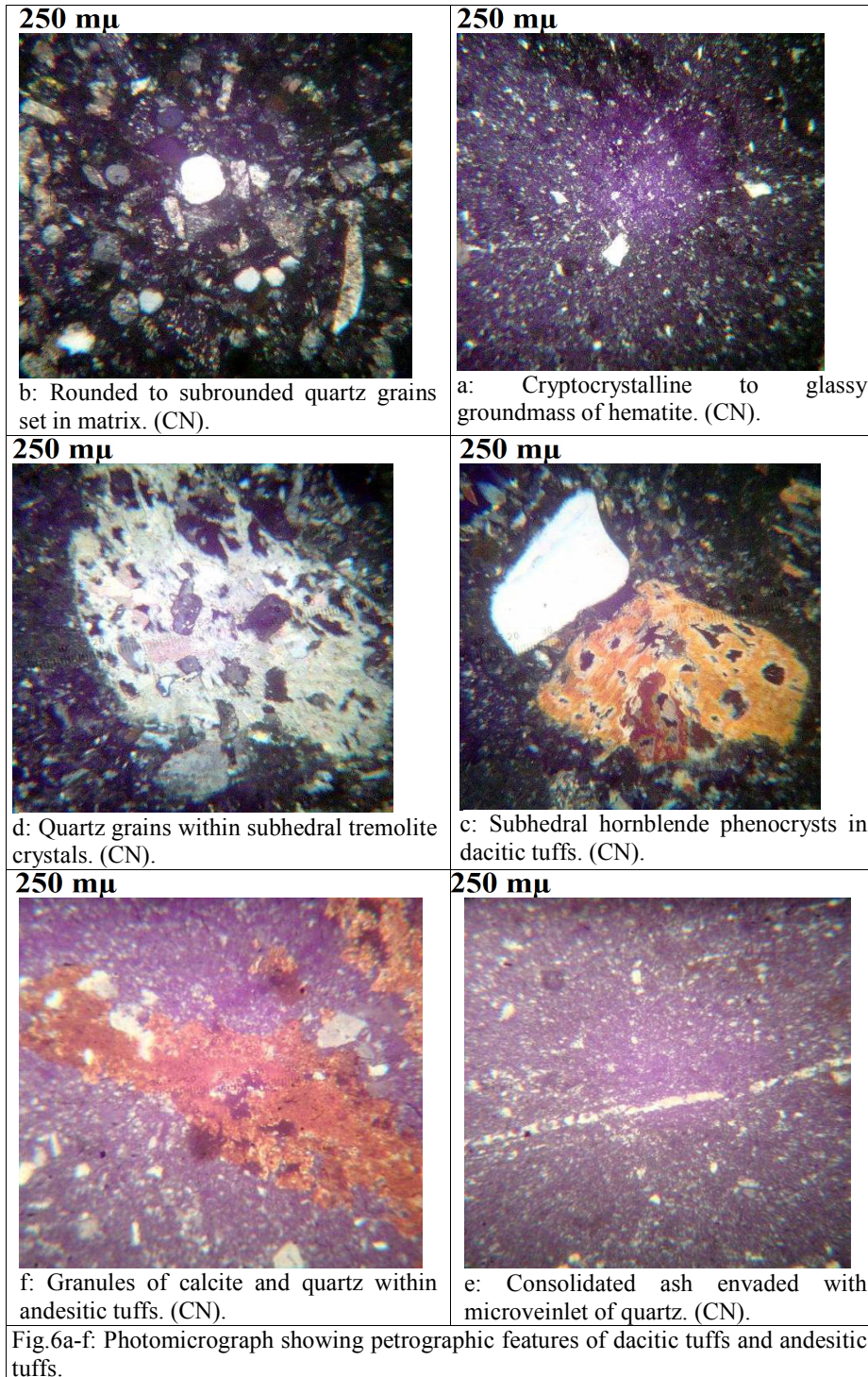
Geochemical characteristics of major oxides and trace elements

Rhyolites and spherulitic rhyolites

Ten samples of the rhyolites and spherulitic rhyolites were analyzed in an attempt to determine their geochemical characteristics (**Table 1**). Major oxides geochemistry indicates that the rhyolites and spherulitic rhyolites are deficient in MnO, FeO, P₂O₅, TiO₂ and MgO; high in Na₂O, K₂O and LOI; and low to high in CaO, Fe₂O₃ contents. From **Table 4** it is clear that the rhyolite rocks have a limited range of SiO₂ contents that varies from 72.10 to 75.20% with an average 73.18% which is relatively lower than the average value of rhyolites by **El-Gaby et al. (1989)**.

The trace element contents of the rhyolites and spherulitic rhyolites show that these rocks contain low concentrations of Zn, Zr, Sr and Pb, whereas those of Y, Ga, Rb and Ba are relatively high (**Table 4**).





The large ion lithophile elements (LILE_s) are concentrated in plagioclase and potash feldspar, respectively (Nockolds and Allen, 1956; Berlin and Henderson, 1969). With regard to ionic radius and charge Ba and Rb can substituted for K, whereas Sr replaces both Ca and K. Consequently, Sr is expected

to be concentrated in the later phases of the plagioclase feldspars and together with Ba in the early phases of the potash feldspars. Rb enters late in the lattice of potash-bearing minerals.

The maximum concentration of Sr in acidic igneous rock series and consequently the depletion of

the crystallizing magma in Sr would start earlier than in Ba (**El-Gaby, 1975**). The uniformity in the distribution of the elements, and the fact that the elements show a variety of important low ratios suggest the nature of the magmatic processes that produced the rhyolites. For instance, the results of the analyses show low contents of Cr, Ni, Cu, Sr and V.

Rhyodacites and dacites

The chemical analyses of these volcanics reveal that SiO₂ ranges from 65.35 to 67.54% for rhyodacite. Al₂O₃ content is relatively higher in dacite (ranges from 15.11 to 15.40%) than the rhyodacite (ranges from 12.01 to 13.84%). CaO content is relatively higher in rhyodacite (ranges from 5.20 to 5.74%); while in dacite is lower and ranges from 3.57 to 3.87%. Na₂O is relatively higher content in dacite (ranges from 4.15 to 4.94%) than the rhyodacite (ranges from 3.03 to 3.78%).

Striking feature of the analyzed rhyodacite is the values of Fe₂O₃ which are mostly higher than those of FeO. The high values of Fe₂O₃ may be attributed to alteration (**Table 2**).

The average of major oxides of the studied rhyodacites is compared with the average of rhyodacites of Gabal Dokhan area (**Basta et al., 1980 and LeMaitre, 1976**) as given in **Table 4**. It is clear that the averages of the studied rhyodacite show relatively higher contents in Fe₂O₃, CaO and Al₂O₃ and lower in SiO₂, FeO and K₂O than those of the rhyodacites of Gabal Dokhan.

The compatible trace elements Cr, Ni and Co, which is generally incorporated in ferromagnesian minerals, generally decreases with increasing differentiation. However, the mean content of Cr in dacites is lower than in Wadi Queh dacites (**Table 4**). Though Cu content shows a wide range of variation, yet a general decrease with increasing differentiation is discernible. Zinc content gently decreases from in Wadi Queh. Both Zr and Y contents increase substantially in dacites, a feature pertinent to within-plate alkaline silicic igneous rocks (**Bowden and Turner, 1974**). The large ion lithophile elements (LILEs) Ba, Rb and Sr are essentially concentrated and related to feldspars.

Bedded dacitic tuffs and andesitic tuffs

Major Oxides Geochemistry: The major oxides for the bedded dacitic and andesitic tuffs are presented in **Table 3**. The tuffs are characterized by SiO₂ contents ranging from 63.54 to 66.43-wt%, with mainly low values of TiO₂ ranging from 0.14 to 0.60 wt%. Fe₂O₃ contents vary from 0.64 to 6.40 wt% and occur in two modes: low (0.64-2.67 wt %) and high (5.12 to 6.40 wt %). FeO abundance levels range from low (1.96%) to high (3.23 %). Na₂O (2.64-3.83 wt %) and K₂O (1.83-3.28 wt %) contents are high; MnO and P₂O₅ contents are very low. All samples

have high LOI (2.91-3.71 wt %) and Al₂O₃ (12.21-15.31 wt %) contents. Very high CaO (3.73-7.02 wt %) are recorded in all the samples. The particularly low MgO suggests that these samples might not contain a significant component of liquidus hypersthene. The behavior of the concentrations of major oxides indicates differential in their level of fractionation of pyroxene during evolution from a single source.

The SiO₂, TiO₂, MnO, P₂O₅ and Na₂O contents of the present volcanic tuffs are comparable with the average of Sai Kung tuffs as given by **Strange, et al. (1990)**, whereas Al₂O₃, K₂O and FeO contents are relatively lower and Fe₂O₃, CaO and MgO contents are higher (**Table 4**).

Trace Element Geochemistry: The trace element compositions of the tuffs show variable ranges, which lie within the compositions for intermediate and acidic rocks. The immobile elements in tuffs show relatively low contents of the Ni and Cr and relatively high contents of the Zr and Nb. Low contents of large cations (Rb, Pb, V and Sr) and high concentrations of Y, Ba, Zn and Ga. In general, the base metals Pb, Zn and Cu show limited variations.

Harker variation diagrams

Harker variation diagrams shows decreasing of TiO₂, Fe₂O₃, FeO, MgO, CaO, Y, Zr, Nb, Sr, Zn and Rb; and increasing Al₂O₃, K₂O, Na₂O, Ba, Cu, Pb and Ga with increasing SiO₂ (Fig.7a, b, c & d). MnO contents are highly variable and significant scatter in Ba, Cr, Ni and V contents is observed.

Petrochemical classification

Several diagrams have been constructed for the petrochemical classification of the investigated Dokhan volcanics as follows:-

On the (Na₂O+K₂O)-SiO₂ binary diagram of **Cox et al. (1979)**, the plotted samples fall in rhyolite, dacite and andesite field (Fig.8a). On the Zr-TiO₂ binary diagram of **Rock (1990)**, the data points of the Dokhan volcanics fall in the rhyolite, dacite and andesite fields (Fig.8b).

The plots of the studied volcanics on the **Taylor** classification diagram revealed that, the Dokhan volcanics are related to rhyolites and dacites (**1969**; Fig.8c). The plots of K₂O against SiO₂ (Fig.8d) is used to classify the volcanic rocks and proposed by **Boillot (1981)**. The studied Dokhan volcanics fall in the rhyolite and dacite fields.

On the Log Zr/TiO₂*0.0001-Log Nb/Y and SiO₂-Zr/TiO₂*0.0001 binary diagrams of **Winchester and Floyd (1977)**, the studied samples fall in and nearby the rhyolite, rhyodacite, trachyte and dacite fields with the exception of six samples which are located in the basanite/nephelinite field due to the high value of Nb/Y ratio (Fig.8e & f).

Table 1: Chemical composition of the rhyolites and spherulitic rhyolites.

| Rock types | Rhyolites | | | | | Spherulitic rhyolites | | | | |
|--------------------------------|-----------|-------|-------|-------|-------|-----------------------|-------|-------|-------|-------|
| | 1Ab | 2Ab | 3Ab | 4Ab | 5Ab | 6Ab | 7Ab | 8Ab | 9Ab | 10Ab |
| Oxides | | | | | | | | | | |
| SiO ₂ | 74.04 | 73.21 | 72.10 | 73.10 | 73.46 | 75.20 | 74.98 | 74.02 | 74.55 | 74.22 |
| TiO ₂ | 0.02 | 0.10 | 0.11 | 0.02 | 0.04 | 0.15 | 0.11 | 0.19 | 0.12 | 0.13 |
| Al ₂ O ₃ | 12.60 | 13.31 | 13.32 | 13.90 | 13.77 | 12.20 | 12.18 | 12.87 | 12.27 | 12.26 |
| Fe ₂ O ₃ | 1.20 | 1.31 | 1.90 | 1.17 | 1.15 | 2.01 | 2.14 | 2.57 | 2.88 | 2.21 |
| FeO | 0.85 | 0.87 | 0.98 | 0.81 | 0.83 | 0.74 | 0.76 | 0.67 | 0.87 | 0.84 |
| MnO | 0.03 | 0.04 | 0.01 | 0.05 | 0.02 | 0.06 | 0.09 | 0.05 | 0.08 | 0.04 |
| MgO | 0.50 | 0.50 | 0.40 | 0.45 | 0.12 | 0.60 | 0.69 | 0.59 | 0.67 | 0.63 |
| CaO | 1.10 | 1.27 | 1.20 | 1.22 | 1.60 | 1.01 | 1.09 | 1.21 | 1.32 | 1.12 |
| Na ₂ O | 3.90 | 4.40 | 4.30 | 4.20 | 4.19 | 4.20 | 4.22 | 4.18 | 4.11 | 4.32 |
| K ₂ O | 3.85 | 3.90 | 3.80 | 3.54 | 3.41 | 3.60 | 3.66 | 3.79 | 3.84 | 3.67 |
| P ₂ O ₅ | 0.04 | 0.05 | 0.06 | 0.02 | 0.01 | 0.06 | 0.03 | 0.09 | 0.04 | 0.05 |
| LOI | 1.59 | 0.80 | 1.10 | 1.49 | 1.34 | 0.60 | 0.54 | 0.32 | 0.11 | 0.61 |
| Total | 99.72 | 99.76 | 99.28 | 99.97 | 99.94 | 99.6 | 100.5 | 100.5 | 100.9 | 100.1 |
| Trace elements (ppm) | | | | | | | | | | |
| Cr | 33 | 35 | 22 | 24 | 32 | 16 | 11 | 14 | 12 | 13 |
| Ni | 15 | 20 | 9 | 18 | 15 | 8 | 6 | 7 | 4 | 5 |
| Cu | 14 | 16 | 10 | 13 | 12 | 12 | 13 | 18 | 17 | 10 |
| Zn | 34 | 48 | 54 | 39 | 45 | 43 | 49 | 45 | 41 | 48 |
| Zr | 280 | 255 | 388 | 322 | 299 | 300 | 387 | 378 | 318 | 312 |
| Rb | 18 | 21 | 43 | 29 | 39 | 37 | 39 | 34 | 38 | 31 |
| Y | 55 | 127 | 77 | 129 | 174 | 88 | 87 | 89 | 92 | 84 |
| Ba | 390 | 491 | 277 | 298 | 314 | 264 | 257 | 294 | 288 | 281 |
| Pb | 29 | 32 | 44 | 39 | 41 | 64 | 66 | 68 | 71 | 69 |
| Sr | 10 | 9 | 13 | 12 | 11 | 23 | 30 | 24 | 29 | 28 |
| Ga | 48 | 20 | 33 | 37 | 43 | 38 | 31 | 36 | 41 | 32 |
| V | 11 | 17 | 6 | 16 | 14 | 6 | 7 | 8 | 5 | 4 |
| Nb | 51 | 49 | 44 | 42 | 48 | 48 | 49 | 51 | 54 | 44 |

Table 2: Chemical composition of the rhyodacites and dacites.

| Rock types | Rhyodacites | | | | | Dacites | | | | |
|--------------------------------|-------------|-------|--------|--------|-------|---------|--------|--------|--------|-------|
| | 11Ab | 12Ab | 13Ab | 14Ab | 15Ab | 16Ab | 17Ab | 18Ab | 19Ab | 20Ab |
| Oxides | | | | | | | | | | |
| SiO ₂ | 65.35 | 66.31 | 66.54 | 65.85 | 67.54 | 67.28 | 67.55 | 67.32 | 66.98 | 67.21 |
| TiO ₂ | 0.11 | 0.14 | 0.84 | 0.16 | 0.30 | 0.67 | 0.19 | 0.14 | 0.12 | 0.61 |
| Al ₂ O ₃ | 13.71 | 13.84 | 12.01 | 12.35 | 13.38 | 15.40 | 15.20 | 15.27 | 15.11 | 15.32 |
| Fe ₂ O ₃ | 3.60 | 3.03 | 3.22 | 3.58 | 0.59 | 2.16 | 2.87 | 2.56 | 2.32 | 2.14 |
| FeO | 1.92 | 1.32 | 1.85 | 1.75 | 3.36 | 1.05 | 1.11 | 1.54 | 1.34 | 1.07 |
| MnO | 0.12 | 0.11 | 0.16 | 0.14 | 0.16 | 0.02 | 0.05 | 0.06 | 0.08 | 0.04 |
| MgO | 2.02 | 1.78 | 1.99 | 2.09 | 0.84 | 1.58 | 1.25 | 1.38 | 1.82 | 1.49 |
| CaO | 5.30 | 5.20 | 5.44 | 5.74 | 5.33 | 3.68 | 3.87 | 3.69 | 3.74 | 3.57 |
| Na ₂ O | 3.03 | 3.24 | 3.78 | 3.55 | 3.19 | 4.15 | 4.19 | 4.79 | 4.94 | 4.51 |
| K ₂ O | 2.04 | 2.10 | 2.18 | 2.41 | 2.69 | 3.05 | 3.88 | 3.49 | 3.11 | 3.18 |
| P ₂ O ₅ | 0.05 | 0.04 | 0.09 | 0.08 | 0.10 | 0.17 | 0.19 | 0.13 | 0.17 | 0.11 |
| LOI | 2.20 | 2.01 | 2.44 | 2.54 | 2.21 | 0.42 | 0.48 | 0.27 | 0.29 | 0.21 |
| Total | 99.45 | 99.12 | 100.54 | 100.24 | 99.69 | 99.63 | 100.83 | 100.64 | 100.02 | 99.46 |
| Trace elements (ppm) | | | | | | | | | | |
| Cr | 20 | 22 | 19 | 27 | 21 | 19 | 18 | 17 | 20 | 15 |
| Ni | 8 | 7 | 8 | 10 | 9 | 16 | 11 | 14 | 15 | 13 |
| Cu | 11 | 13 | 10 | 14 | 12 | 11 | 10 | 13 | 15 | 14 |
| Zn | 161 | 164 | 162 | 168 | 163 | 18 | 15 | 16 | 19 | 17 |
| Zr | 1119 | 1123 | 1117 | 1113 | 1121 | 324 | 328 | 329 | 343 | 330 |
| Rb | 59 | 58 | 57 | 51 | 57 | 81 | 85 | 87 | 88 | 89 |
| Y | 510 | 514 | 517 | 519 | 515 | 547 | 544 | 549 | 587 | 550 |
| Ba | 460 | 467 | 462 | 461 | 467 | 206 | 239 | 229 | 224 | 212 |
| Pb | 35 | 39 | 31 | 38 | 37 | 58 | 55 | 54 | 59 | 53 |
| Sr | 50 | 54 | 51 | 56 | 52 | 96 | 92 | 93 | 97 | 91 |
| Ga | 37 | 38 | 35 | 34 | 38 | 38 | 37 | 31 | 39 | 34 |
| V | 5 | 4 | 8 | 6 | 7 | 21 | 28 | 22 | 24 | 29 |
| Nb | 210 | 216 | 219 | 218 | 215 | 159 | 156 | 157 | 158 | 153 |

Table 3: Chemical composition of the dacitic tuffs and andesitic tuffs.

| Rock types | Dacitic tuffs | | | Andesitic tuffs | | |
|--------------------------------|---------------|--------|--------|-----------------|-------|-------|
| Oxides | 21Ab | 22Ab | 23Ab | 24Ab | 25Ab | 26Ab |
| SiO ₂ | 65.32 | 66.43 | 64.84 | 62.54 | 62.88 | 63.12 |
| TiO ₂ | 0.14 | 0.60 | 0.26 | 0.22 | 0.27 | 0.24 |
| Al ₂ O ₃ | 13.50 | 15.31 | 13.88 | 12.21 | 13.25 | 12.28 |
| Fe ₂ O ₃ | 5.30 | 0.64 | 2.67 | 6.40 | 5.12 | 5.31 |
| FeO | 3.23 | 2.72 | 1.96 | 2.32 | 2.28 | 2.39 |
| MnO | 0.16 | 0.17 | 0.14 | 0.24 | 0.57 | 0.78 |
| MgO | 1.60 | 1.38 | 2.38 | 1.20 | 1.08 | 1.11 |
| CaO | 5.90 | 3.73 | 4.84 | 7.02 | 6.08 | 6.57 |
| Na ₂ O | 2.90 | 3.69 | 3.83 | 2.66 | 2.67 | 2.64 |
| K ₂ O | 2.30 | 3.28 | 1.83 | 1.90 | 1.89 | 1.99 |
| P ₂ O ₅ | 0.09 | 0.19 | 0.15 | 0.10 | 0.15 | 0.18 |
| LOI | 3.10 | 2.91 | 3.71 | 2.20 | 3.51 | 3.15 |
| Total | 103.54 | 101.05 | 100.49 | 99.01 | 99.75 | 99.76 |
| Trace elements (ppm) | | | | | | |
| Cr | 14 | 15 | 16 | 22 | 27 | 24 |
| Ni | 5 | 6 | 4 | 3 | 8 | 5 |
| Cu | 7 | 8 | 6 | 5 | 6 | 7 |
| Zn | 124 | 127 | 126 | 96 | 97 | 99 |
| Zr | 569 | 570 | 567 | 678 | 680 | 684 |
| Rb | 64 | 65 | 68 | 45 | 51 | 49 |
| Y | 357 | 355 | 387 | 435 | 450 | 466 |
| Ba | 347 | 350 | 355 | 421 | 458 | 444 |
| Pb | 23 | 27 | 29 | 32 | 36 | 38 |
| Sr | 32 | 34 | 33 | 34 | 37 | 39 |
| Ga | 24 | 27 | 26 | 12 | 18 | 20 |
| V | 5 | 8 | 9 | 2 | 4 | 5 |
| Nb | 153 | 155 | 157 | 149 | 155 | 143 |

Table 4: Average compositions of the Dokhan volcanics with some averages of Egyptian and World volcanics.

| Oxides | 1 | 7 | 2 | 3 | 9 | 4 | 8 | 5 | 12 | 6 | 10 | 11 |
|--------------------------------|-------|--------------|-------|-------|--------------|-------|--------------|-------|--------------|-------|--------------|--------------|
| SiO ₂ | 73.18 | 76.12 | 74.59 | 66.32 | 69.69 | 66.27 | 64.67 | 65.53 | 62.33 | 62.85 | 65.01 | 72.82 |
| TiO ₂ | 0.06 | 0.20 | 0.14 | 0.31 | 0.30 | 0.35 | 0.47 | 0.33 | 0.58 | 0.24 | 0.58 | 0.28 |
| Al ₂ O ₃ | 13.38 | 11.49 | 12.36 | 13.06 | 12.95 | 15.26 | 16.03 | 14.23 | 16.73 | 12.58 | 15.91 | 13.27 |
| Fe ₂ O ₃ | 1.35 | 2.65 | 2.36 | 3.36 | 1.16 | 2.41 | 3.43 | 2.87 | 1.19 | 5.61 | 2.43 | 1.48 |
| FeO | 0.87 | -- | 0.72 | 1.71 | 3.78 | 1.22 | -- | 2.64 | 3.40 | 2.33 | 2.30 | 1.11 |
| MnO | 0.03 | 0.05 | 0.06 | 0.14 | 0.08 | 0.05 | 0.09 | 0.16 | 0.15 | 0.53 | 0.09 | 0.06 |
| MgO | 0.39 | 0.22 | 0.64 | 1.74 | 1.12 | 1.50 | 3.14 | 1.79 | 0.10 | 1.13 | 1.78 | 0.39 |
| CaO | 1.28 | 0.54 | 1.15 | 5.40 | 2.58 | 3.71 | 3.31 | 4.82 | 3.22 | 6.56 | 4.32 | 1.14 |
| Na ₂ O | 4.20 | 3.33 | 4.21 | 3.36 | 3.24 | 4.52 | 4.88 | 3.47 | 2.50 | 2.66 | 3.79 | 3.55 |
| K ₂ O | 3.70 | 2.70 | 3.71 | 2.28 | 3.79 | 3.34 | 4.41 | 2.47 | 6.12 | 1.93 | 2.17 | 4.30 |
| P ₂ O ₅ | 0.04 | 0.07 | 0.05 | 0.07 | 0.06 | 0.15 | 0.09 | 0.43 | 0.21 | 0.14 | 0.15 | 0.07 |
| LOI | 1.26 | 2.47 | 0.44 | 2.28 | -- | 0.33 | 3.17 | 3.24 | 1.79 | 2.95 | 1.19 | 1.41 |
| Trace elements (ppm) | | | | | | | | | | | | |
| Cr | 29 | 18 | 13 | 22 | -- | 18 | 154 | 15 | -- | 24 | -- | -- |
| Ni | 15 | 11 | 6 | 8 | -- | 14 | 35 | 5 | -- | 5 | -- | -- |
| Cu | 13 | 12 | 14 | 12 | -- | 13 | 35 | 7 | -- | 6 | -- | -- |
| Zn | 44 | 108 | 45 | 164 | -- | 17 | 57 | 126 | -- | 97 | -- | -- |
| Zr | 309 | 769 | 339 | 1119 | -- | 331 | 172 | 569 | -- | 681 | -- | -- |
| Rb | 30 | 11 | 36 | 56 | -- | 86 | 16 | 66 | -- | 48 | -- | -- |
| Y | 112 | 96 | 88 | 515 | -- | 555 | 22 | 366 | -- | 450 | -- | -- |
| Ba | 354 | 281 | 277 | 463 | -- | 222 | 1004 | 351 | -- | 441 | -- | -- |
| Pb | 37 | 110 | 68 | 36 | -- | 56 | 21 | 26 | -- | 35 | -- | -- |
| Sr | 11 | 76 | 27 | 53 | -- | 94 | 446 | 33 | -- | 37 | -- | -- |
| Ga | 36 | 27 | 36 | 36 | -- | 36 | 20 | 26 | -- | 17 | -- | -- |
| V | 13 | -- | 6 | 6 | -- | 25 | -- | 7 | -- | 4 | -- | -- |
| Nb | 47 | -- | 49 | 216 | -- | 157 | -- | 155 | -- | 149 | -- | -- |

1. Average of the studied rhyolites. 2. Average of the studied spherulitic rhyolites. 3. Average of the studied rhyodacites.

4. Average of the studied dacites. 5. Average of the studied bedded dacitic tuffs. 6. Average of the studied andesitic tuffs.

4. Average rhyolites of Wadi Queh area (El-Gaby *et al.*, 1989). 8. Average dacites of Wadi Queh area (El-Gaby *et al.*, 1989).

9. Average rhyodacites of Gabal Dokhan area (Basta *et al.*, 1980). 10. Average of 578 dacites (LeMaitre, 1976).

11. Average of 554 rhyolites (LeMaitre, 1976). 13. Average tuffs of Sai Kung and Clear Water Bay Formation within Tai Miu Wan Member (Strange, *et al.*, 1990).

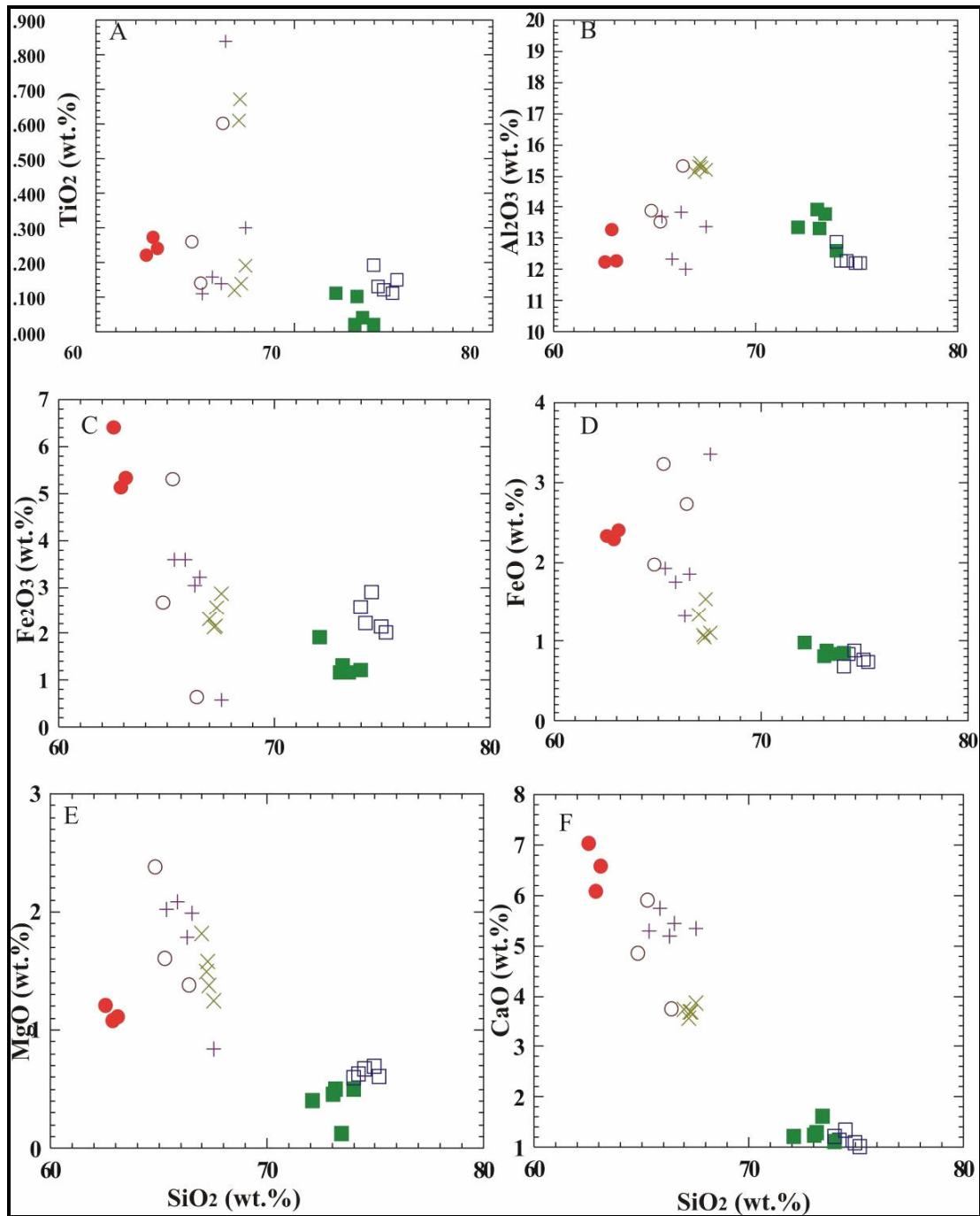


Fig.7a: Harker variation diagram of SiO₂ versus major oxides for the studied Dokhan volcanics.

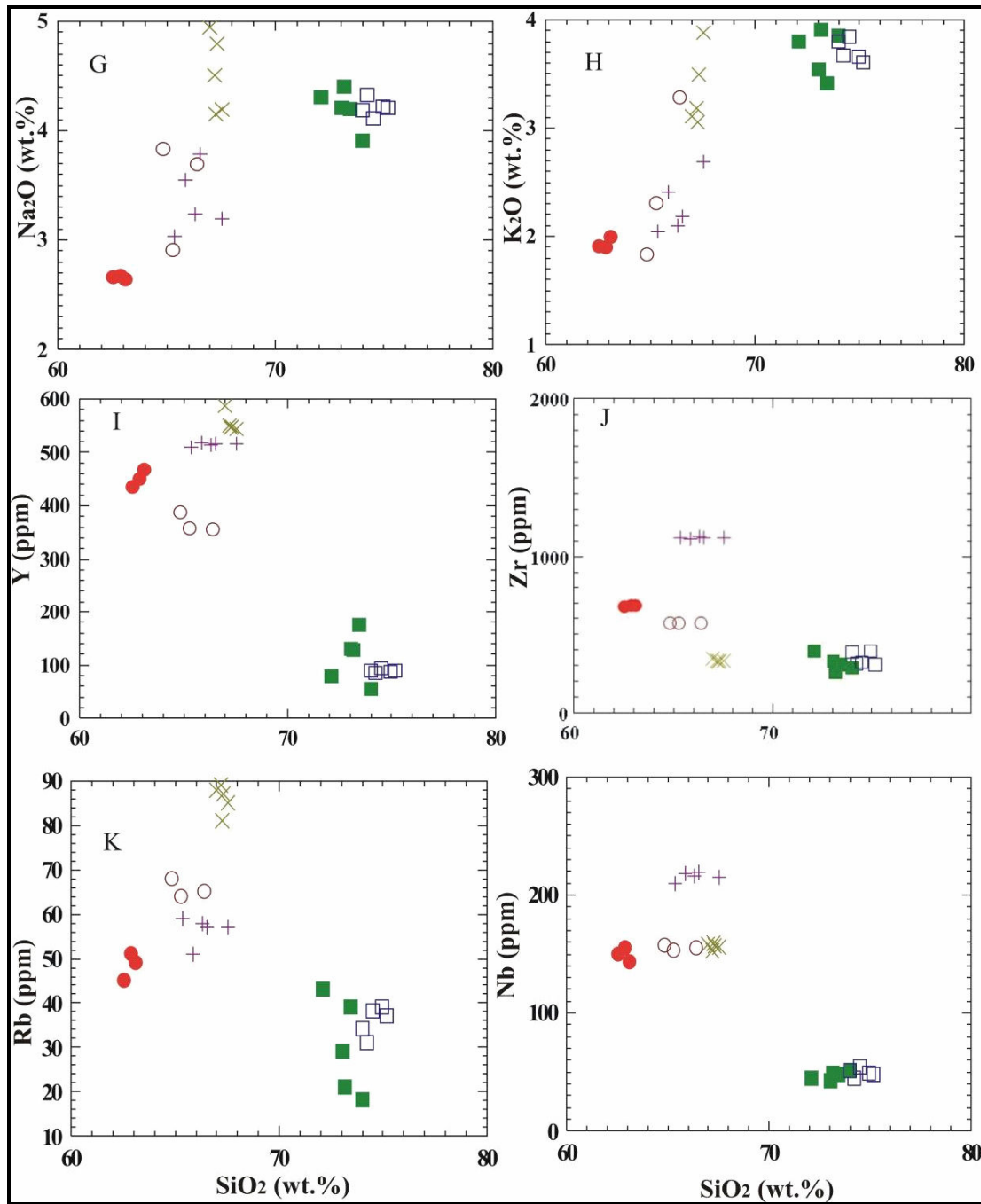


Fig.7b: Harker variation diagram of SiO₂ versus major oxides and trace elements for the studied Dokhan volcanics.

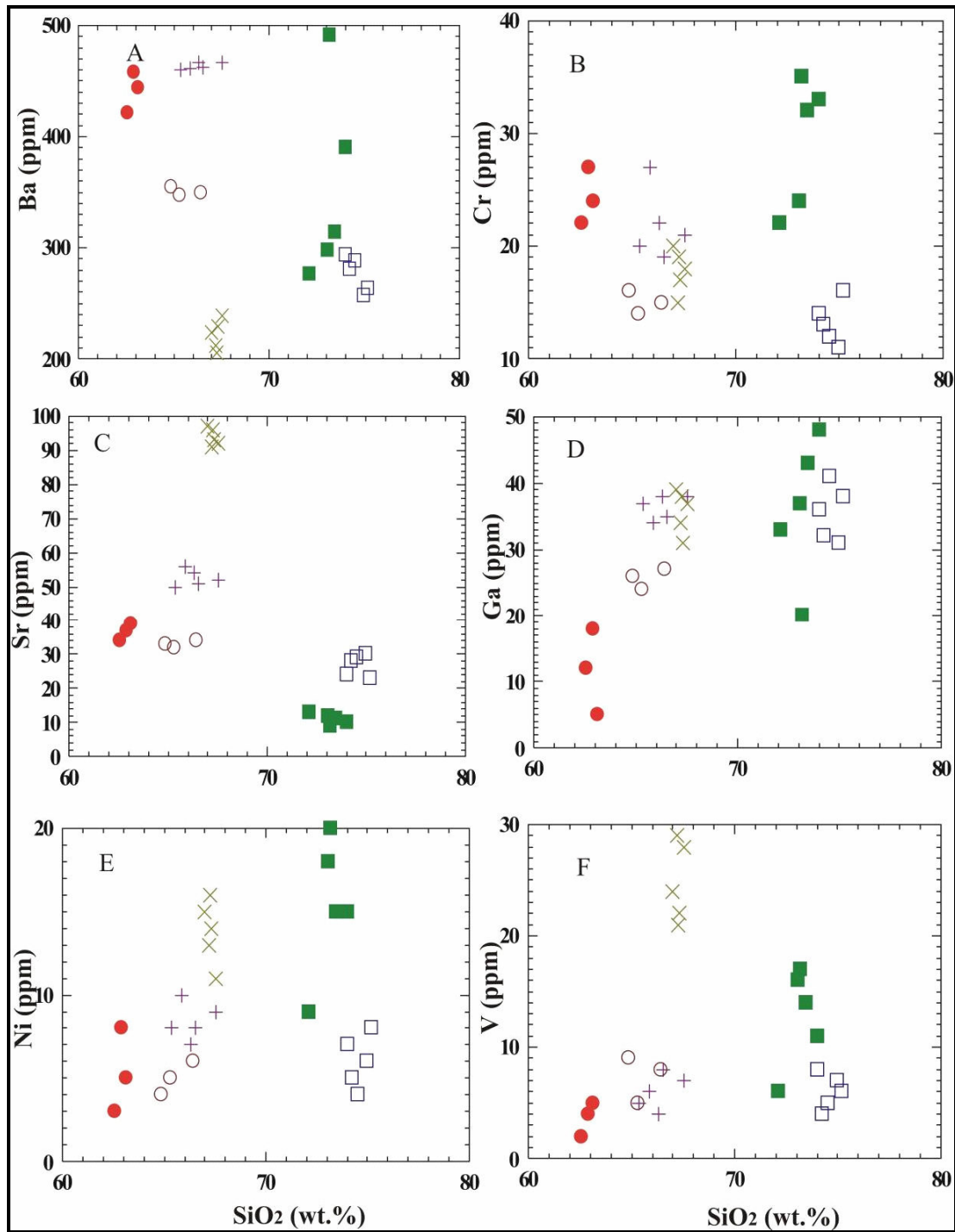


Fig.7c: Harker variation diagram of SiO₂ versus trace elements for the studied Dokhan volcanics.

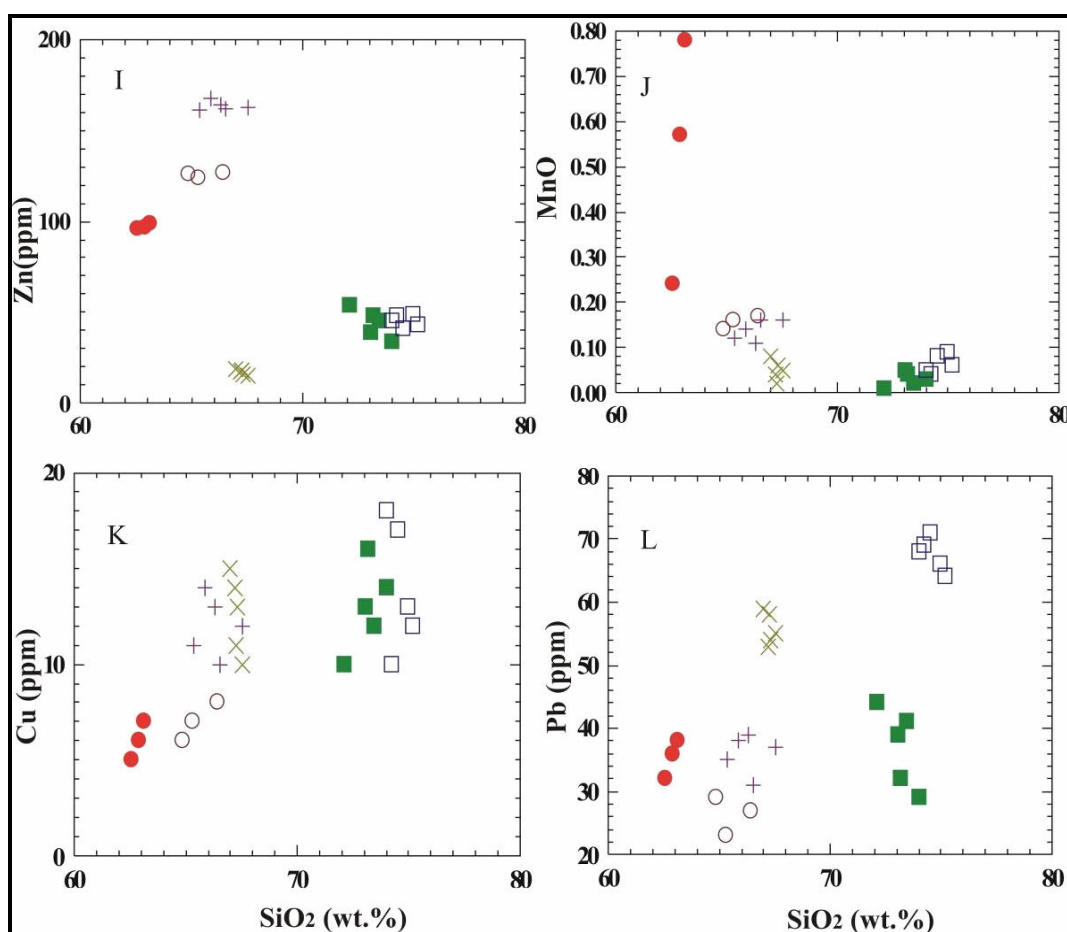


Fig.7d: Harker variation diagram of SiO₂ versus trace elements for the studied Dokhan volcanics.

Magma type

The values of total alkalis and silica of the rhyolites are plotted on the proposed (TAS) diagram of **Irvine and Baragar (1971)**. It is clear that, the studied volcanics are subalkaline affinity, indicating that, they are the product of anorogenic tectonic environment (Fig.9a). The data points of the studied volcanic rocks on this AFM ternary diagram (Fig.9b) of **Irvine and Baragar (1971)** fall in calc-alkaline field with tendency to be of tholeiite nature. This diagram shows also that, the samples are markedly enriched in alkalis and depleted in iron and magnesium contents.

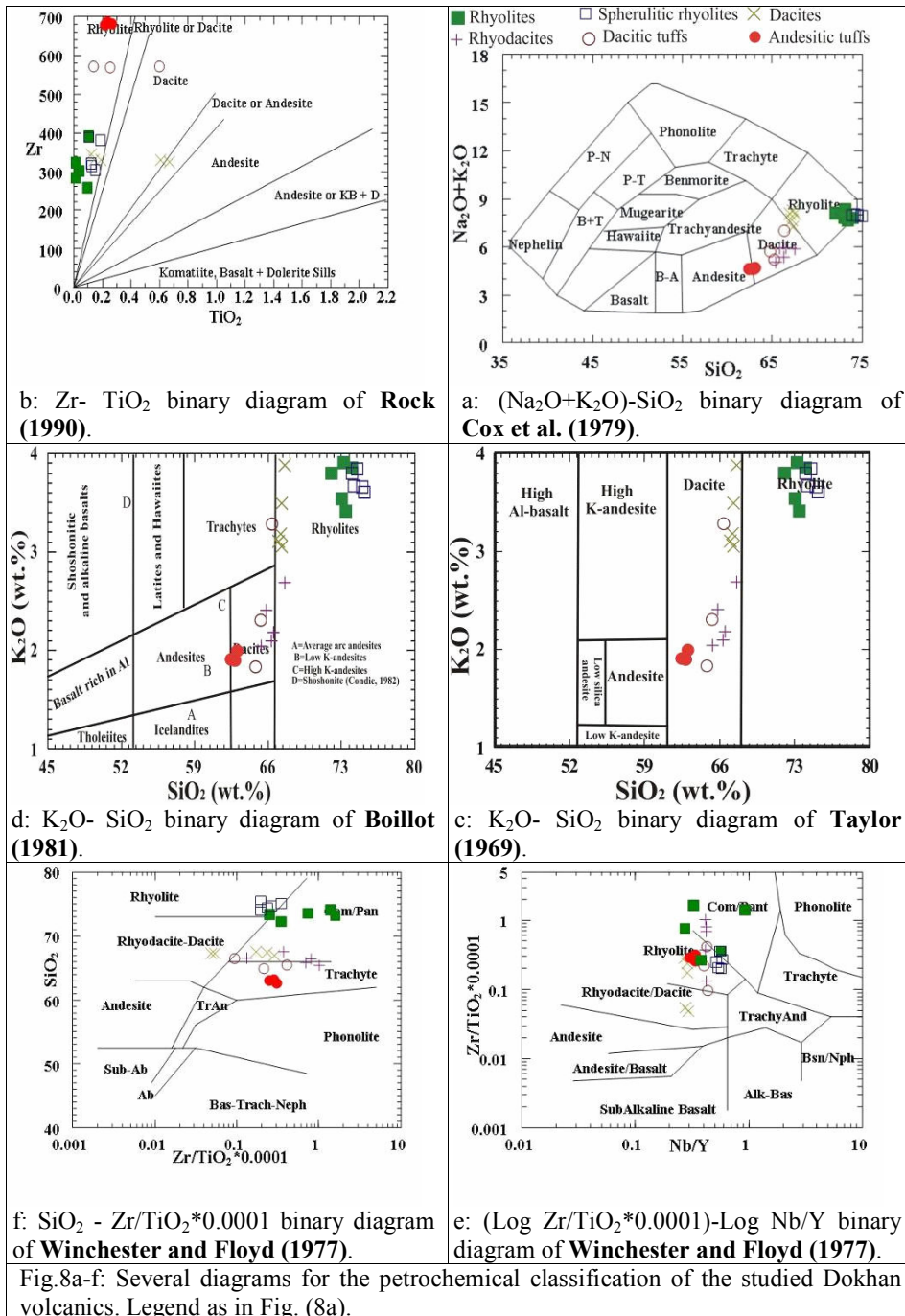
The $\text{Al}_2\text{O}_3/(\text{Na}_2\text{O}+\text{K}_2\text{O})$ versus $\text{Al}_2\text{O}_3/(\text{CaO}+\text{Na}_2\text{O}+\text{K}_2\text{O})$ diagram of **Maniar and Piccoli (1989)** shows that all samples of the studied Dokhan volcanics are metaluminous except three samples of rhyolite which exhibits peraluminous nature (Fig.9c). **Miyashiro (1973)** proposed the SiO₂ versus (FeO*/MgO) binary diagram to differentiate between the calc-alkaline and tholeiite of the magma. The analyzed samples plot in the calc-alkaline field (Fig.9d).

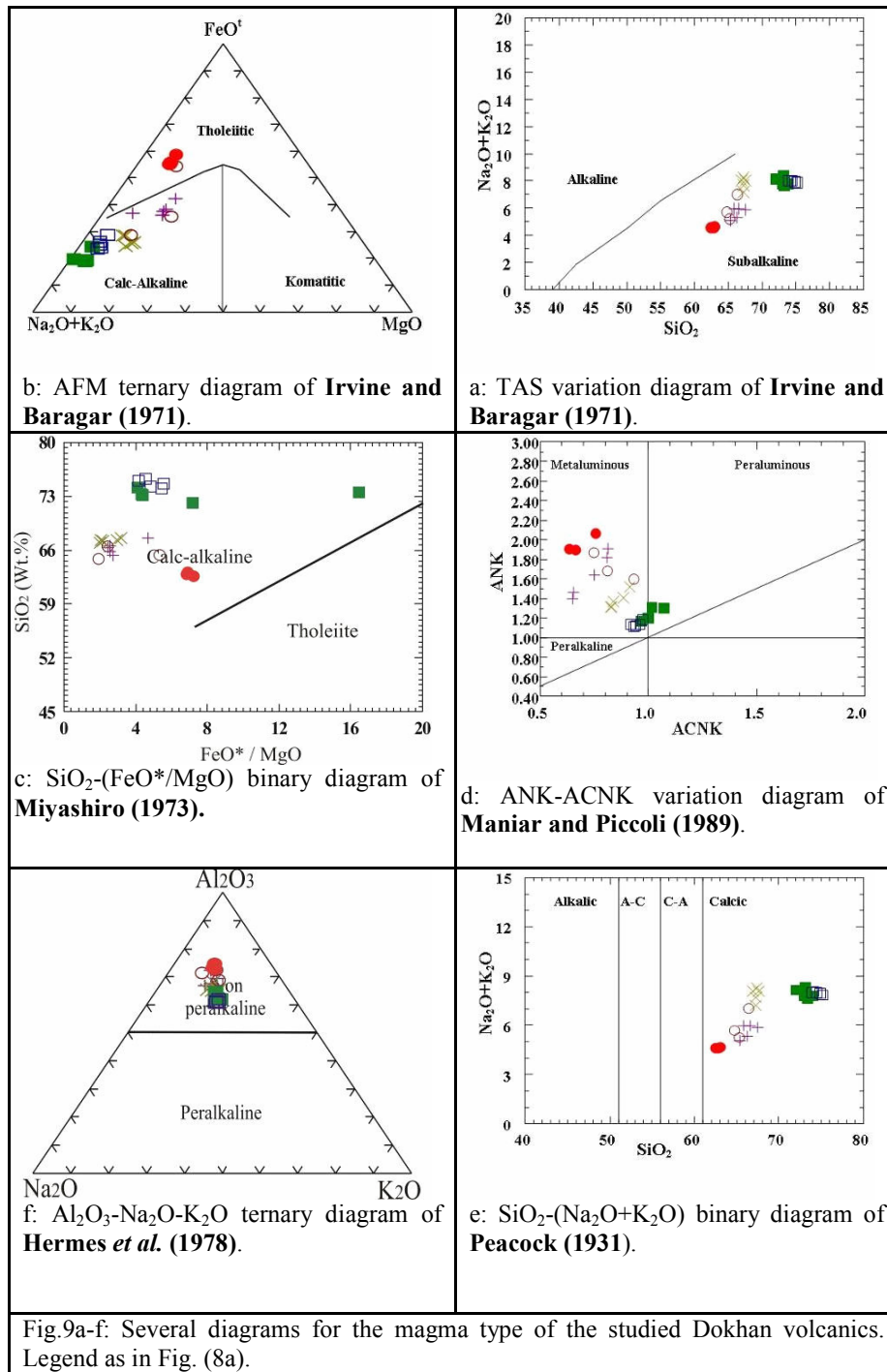
The studied samples plotted on the (Na₂O+K₂O)-SiO₂ binary diagram of **Peacock (1931)** show that they fall in the calcic field (Fig.9e). Figure (9f) shows the fields of non-peralkaline and peralkaline volcanics using the Al₂O₃-Na₂O-K₂O ternary diagram of **Hermes et al. (1978)**. On this diagram, all the data points of the studied Dokhan volcanics fall in non-peralkaline field.

Petrogenesis

There are several ways for petrogenetic volcanisms in which mantle-derived magmas may interact with crustal rocks (**Huppert and Sparks 1985**):-

- Partial melts from crust and mantle sources may mix in magma chambers or conduits.
- The walls, roof and floor of a magma chamber (or the walls of conduits) may begin to melt, when their solidus temperature is exceeded and in fluid dynamically favorable circumstances, this melt can contaminate the magma chamber by mixing.
- Blocks of wall rocks can be stopped into the magma and assimilated by complete melting (bulk assimilation).





The volcanics apparently do not represent one phase of whole some crystallization and differentiation; batch melting and crystallization appear to have been prevalent, given the elemental spread.

The origin and evolutionary of rhyolitic magmas have been attributed to six major processes by **Raymond (2002)**:- 1. Anatexis of rocks in the mantle, either mantle rocks or transported into the mantle by tectonic processes; 2. Fractional

crystallization of basaltic or other magmas; 3. Anatexis of crustal rocks; 4. Assimilation accompanied by fractional crystallization; 5. Magma mixing with fractional crystallization, and 6. Fractional or melting followed by liquid state thermogravitational. **Ringwood (1974)** suggested that rhyolitic magma formed by partial melting of quartz eclogite, as a part of this model for arc-basaltic petrogenesis. Eclogite is produced at mantle depths by metamorphism of basaltic oceanic crust during subduction.

This process was investigated via experimental melting studies conducted by **Huang and Wyllie (1981)**, which indicate that primary melt can not be generated at mantle depths by anatexis of either mantle rocks or subducted oceanic crust.

The trace element patterns of the **rhyolite and spherulitic rhyolite** samples reflect melts from same source. The normalized multi-element distribution patterns of the rhyolite and spherulitic rhyolite rocks of the Dokhan volcanics (Fig.10a, b and c) show that the calc-alkaline suites have low (Zn, Sr, V, Cr, Ni, Cu and Pb) and high (Nb, Rb, Zr, Y, Ba, Ga and Hf) contents, which are characteristic of continental type crust and immature island arc.

From all the above mentioned discussion, it is clear that the magma of these volcanic rocks have been derived by fractional or melting followed by liquid state thermogravitational process (**Hildreth, 1981**). The process involves thermal and convection driven chemical processes that enrich the roof of the magma chamber in volatiles, promoting chemical distribution of elements and the formation of high silica rhyolites.

The chondrite-normalized spider-diagrams of **rhyodacite and dacite** are characterized by high concentration of some high field strength elements (HFSEs) Zr, Y, Ba, Nb and depletion in large ionic lithophile elements (LILEs) Rb, Cr, Ni, Cu, V. The high concentration of Zr, Y, Ba and Nb may be due to the presence of zircon and apatite during partial melting. The pronounced negative Nb anomalies among the studied rhyodacite and dacite samples may have been caused either by the low solubility of HFSEs with respect to LILEs in hydrous fluids (**McCulloch and Gamble, 1991**) or by the presence of ilmenite phase, which may have been stabilized under water-rich conditions (**Sunders et al., 1980**).

The narrow range of the concentrations of incompatible elements such as Zn and Ni indicates homogeneity in incompatible elements in source material.

The low Ni and Cr contents do not necessarily

suggest that the magma fractionated strongly because the positive correlation between Ni and Cr is an indication of their occurrence in liquidus phase. It is apparent that the low contents of Ni, Cu, Sr, V and Cr in the rocks indicate source characteristics and some degree of fractionation of magnetite, ilmenite diopside and hypersthene.

The trace element patterns of **bedded dacitic tuffs and andesitic tuffs**, normalized to chondritic meteorites show enrichment of the HFSE relative to the LILE except two elements of Ba and Rb is high concentration and the consistency of the HFSE and irregularity in the pattern of concentrations of LILE (Figure 10a, b and c). Parental magma to the andesitic tuffs may have followed a single fractional crystallization path controlled by batch melting and scaled fractionation of hornblende and tremolite during magma ascent.

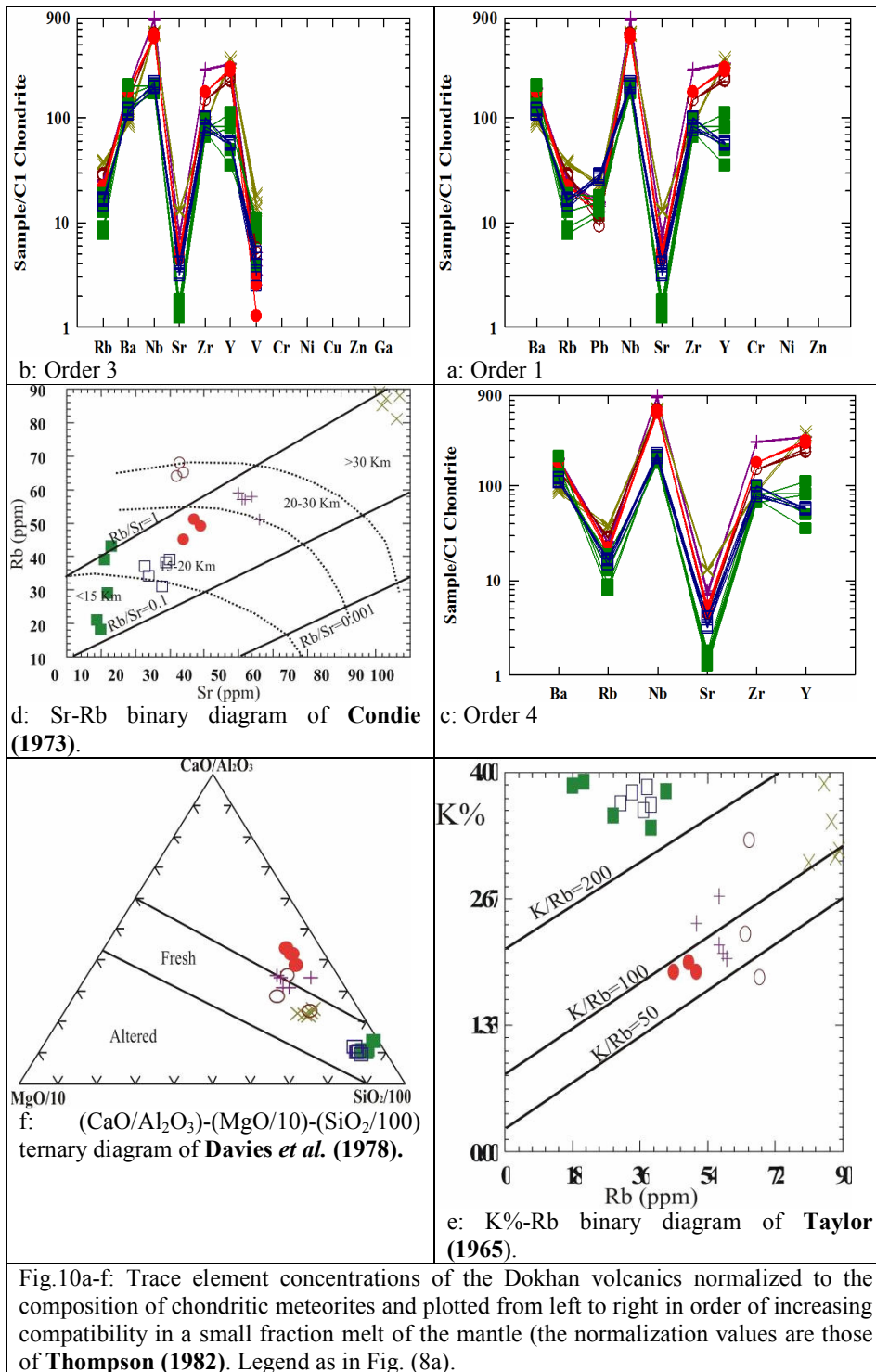
Rb-Sr variation diagram given by **Condie (1973)** shows Rb-Sr crustal thickness index. The plots of spherulitic rhyolite, andesitic tuffs and dacitic tuffs on this diagram indicate that they were formed at crustal thickness in the range of 20-30km. On the other hand, dacites formed at crustal thickness more than 30km (Fig.10d). The plots of the studied rhyolites on this diagram indicate that they are formed at crustal thickness less than 15km.

The studied samples are plotted in the K-Rb diagram as shown in Fig. (10e). It is clear from the diagram that the points are encountered in the region of crustal rocks as suggested by **Taylor (1965)**. The plotted rhyolites and spherulitic rhyolites are restricted above the line of $K/Rb=200$. Also, there is a general negative correlation between K and Rb. The Rb contents (86 ppm) are considerably higher than those which might be expected in the Wadi Queh dacites (16 ppm in Table 4). Most of the plotted dacite, rhyodacite, andesitic and dacitic tuffs are distributed between the lines of $K/Rb=50$ and $K/Rb=100$.

The impact of the hydrous fluids on the volcanic rocks might be estimated by using the method of **Davies et al. (1978)** on the ternary diagram $MgO/10-SiO_2/100-CaO/Al_2O_3$ as shown in Fig.10f. Most of the data points of the studied Dokhan volcanic fall in the field of fresh volcanics.

Tectonic Environments

The tectonic environments of the Dokhan volcanics are discussed by many authors. The geochemical studies indicate that they are calc-alkaline orogenic complex of island arc with continental type crust (**Gass, 1982**) or Andean type continental margins (**El-Gaby et al., 1990**).



There are three various models are suggested for the emplacement of the Dokhan volcanics.

- The Dokhan volcanics eruptions are related to a period of strong extension (anorogenic) analogous

to that of the Oslo rift (**Stern and Gottfried, 1986**).

- The Dokhan volcanics were interpreted to have been formed in a transitional environment

between compressive and extensional tectonic settings (**Ressetar and Monard, 1983**).

- Dokhan volcanic is a subduction-related environment of compressional tectonic setting (**Abdel Rahman, 1996**).

Ewart (1979 & 1981) has reviewed the lava analyses from various modern geotectonic settings and gave average abundances of thirty minor and trace elements from the main volcanic environments and suggests the following geotectonic settings:-

- 1- Active continental margins (Western USA and Andean South America).
- 2- Anorogenic environments (Iceland, South East Queensland and Western Scotland-Northern Ireland Province).
- 3- Oceanic island (Galapagos, Hawaii, Canaries and the Zephyr Shoal).
- 4- Primitive ensimatic island arcs (Tonga-Kermadec and Lesser Antilles).

On the basis of tectonic setting **Wilson (2007)** can define four distinct environments in which volcanics may be generated:-

- (1) Constructive plate margins: These divergent plate boundaries include the system of mid-oceanic ridge volcanics and back-arc spreading center volcanics.
- (2) Destructive plate margins: These convergent plate boundaries include island arc volcanics and active continental margin volcanics.
- (3) Oceanic intra-plate settings: Oceanic island volcanics.
- (4) Continental intra-plate settings: Including continental flood basalt provinces, continental rift zones and occurrences of potassic and ultrapotassic magmatism (including kimberlites) not related zones of rifting.

Ressetar and Monard (1983) noted that the Dokhan lava had elevated concentrations of incompatible trace elements with respect to igneous rocks, typical of active continental margins.

Heikal and Ahmed (1984) believed that the Dokhan volcanics are erupted on mature island arcs with continental-type crust.

Volcanic rocks, exhibit specific chemical features for specific tectonic environments (**Pearce and Cann, 1973 and Wood et al., 1979**). The tectonic environment of the studied Dokhan volcanics is clarified on various discrimination diagrams, to compare the studied volcanics with some well known various tectonic settings.

The CaO-Na₂O-K₂O ternary diagram (Fig.11a) shows that these Dokhan volcanics are of active continental margin (rhyolite) and continental island arc (dacite; **Rollinson, 1993**).

Miyashiro and Shido (1975) proposed use of Cr-FeO*/MgO discrimination tectonic diagram. The plots of the studied Dokhan volcanics on this diagram

(Fig.11b), show that they fall mostly within the field of volcanic rocks of island arc and active continental margin.

On the Nb-SiO₂ binary diagram (Fig.11c) of **Pearce and Gale (1977)**, elucidate that most of the studied volcanics fall in the within plate field, whereas, the rhyolite and spherulitic rhyolite samples lie in the crustal melt.

Ewart (1979 & 1981) suggested various discrimination diagrams to identify the modern tectonic environments. The plots of studied Dokhan volcanic samples on SiO₂ versus Zr binary diagram, indicate that, most samples fall within active continental margin and anorogenic volcanic terrains (Fig.11d).

On the FeO*-MgO-Al₂O₃ discriminated diagram (Fig.11e) of **Pearce et al. (1977)**, the plotted samples form a tight cluster and lie in the spreading centre island and island arc and active continental margin fields.

The plotted samples on the K₂O/Na₂O-SiO₂ discrimination diagram (Fig.11f) of **Roser and Korsch (1986)**, show that the majority of the points are distributed in the field of active continental margin (ACM) and passive continental margin (PCM) except one sample lie in the island arc field; this variation is due to variable contents of K₂O/Na₂O and SiO₂.

Discussion and Conclusions

The geologic, petrographic and major element geochemistry of rhyolites and spherulitic rhyolites from Abu Hamra area suggests that they represent high-K₂O calc-alkaline rhyolites, which resulted from the fractionation of the quartz and plagioclase from a common magma source.

The Geochemical characteristics of the studied dacitic and volcanic tuffs revealed their calc-alkaline nature with a rather tholeiitic affinity. The chondrite-normalized spider-diagrams and the tectonic setting discrimination diagrams constantly reflect their continental margin arc setting.

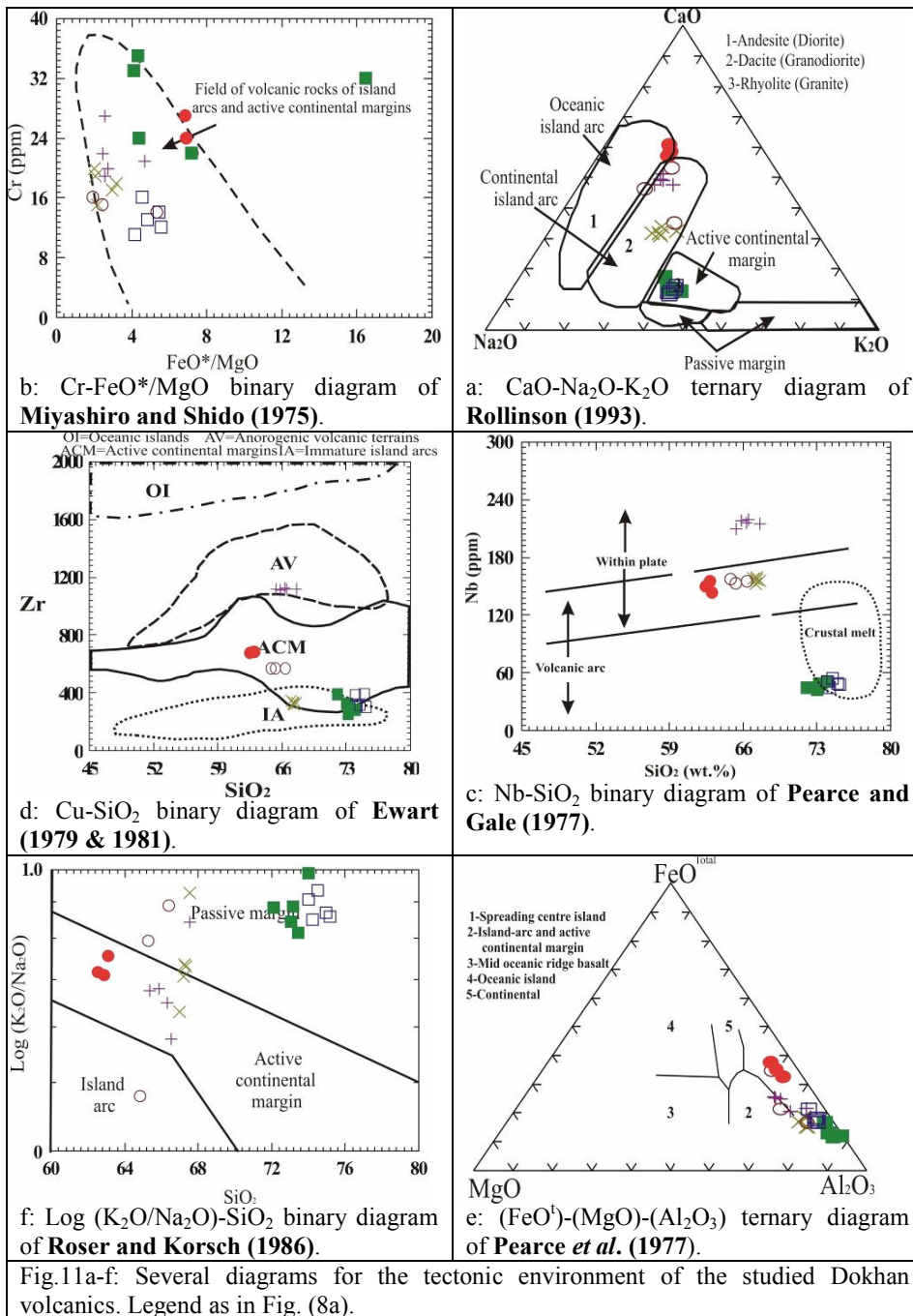
Geochemical values of immobile trace elements (Zr, Y and Nb) and low ratios of Ba/Nb suggest that the protolith was emplaced as volcanics in a spreading boundary, such as continental margin and within plate volcanics WPV setting. Also the affinity to spreading centers is confirmed by very low ratios of Ba/Nb.

Zircon during silicic fractional crystallization

The concentration of Zr is lower in the more evolved rhyolites than in the rhyodacites. In partial melting Zr (an incompatible element) should be concentrated in initial melts (rhyolites and spherulitic rhyolites) and become diluted as melting progresses toward producing dacite (rhyodacites and quartz dacites).

The rhyolites are then a further fractionation with a lower Zr concentration because zircon became a fractionating phase at the point of dacite development. An alternative explanation is that the dacites are the result of partial melting that then

fractionated zircon as the rhyolite is produced. Major changes in the composition of erupted magmas at each type of the Dokhan volcanic activity can be related to variations in the degree of partial melting in the upper mantle.



The Dokhan volcanics appear to be within plate and continental rift volcanic piles dominated by calc-alkaline magmatism during the development of a proto-sea in the Northeast Africa. The plot of most samples in the field of active continental margin and within plate volcanism is consistent with their composition and therefore, depicts their tectonic setting. It is apparent the island arc affinity is related to the initial magmatic source, while the continental affinity characterizes a later emplacement in a sediment-dominated spreading environment. In other words, their intrusion was initiated beneath spreading centers and later migrated to a continental spreading setting. From the discussions above, the likely petrogenetic and geotectonic model is that these tuffs constitute calc-alkaline volcanism emplaced in a within plate setting and subsequently rested on a continental rift setting.

Tectonically, rhyolites and spherulitic rhyolites seem to have evolved in an active continental margin, non-orogenic intraplate magma (WP) and possibly representing the stage of island arc volcanic setting. The rhyodacites and dacites were developed in anorogenic volcanic terrains and active continental margin. The bedded dacitic tuffs and andesitic tuffs developed either in an active continental margin or within plate volcanics and in spreading centre tectonic settings.

This study has therefore shown that calc-alkaline volcanism was generated from continental spreading setting and that the volcanism eventually extended to continental rift setting when drifting and supply of magma continued from depth under the Egyptian Desert. The whole-rock and mineral compositions of Abu Hamra Dokhan volcanic rocks suggest a complex differentiation history within the continental crust.

During fractional or melting followed by liquid state thermogravitational process exchange of elements with the wall rocks occurs around the chamber margins. A temperature gradient from low temperature near the top and sides to high temperature at the base and center exists in the magma chamber giving the primary cause of the convection. Early eruption phases will yield high silica rhyolites and spherulitic rhyolites from the top of the magma chamber and these rocks will blanket the ground first. Later eruptive phases successively yield rhyodacites and dacites and the final phases forming successive bedded dacitic tuff and andesitic tuff layers.

Corresponding author:

Hatem M. El-Desoky,
Department of Geology, Faculty of Sciences, Al-Azhar University, Cairo, Egypt, Email hatem_eldesoky2002@yahoo.com

References

1. **Abdel Rahman A.M. (1996).** Pan-African volcanism: petrology and geochemistry of the Dokhan Volcanic suite in the northern Nubian Shield. *Geol Mag* 133:17–31.
2. **Akaad, M.K. and Abu El-Ela, A.M. (2002).** Geology of the Basement Rocks in the Eastern Half of the Belt between Latitudes 25°30' and 26°30'N, Central Eastern Desert, Egypt. *Geol. Surv.*, paper No. 78.
3. **Basta, E.Z., Kotb, H. and Awadalla, M.F. (1980).** Petrochemical and geochemical characteristics of the Dokhan Formation at the type locality, Jabal Dokhan, Eastern Desert, Egypt. *Inst Appl. Geol Jeddah Bull* 3:121–140.
4. **Berlin, R. and Henderson, C.M.B. (1969).** *Geochim Cosmochim. Acta*, 33, 247-55.
5. **Boillot, G. (1981).** Geology of the continental margins. Longman London, 115pp.
6. **Bowden, P. and Turner, D.C. (1974).** Peralkaline and associated Ring-complexes in the Nigeria-Niger Province, West Africa: In H. Sorensen (ed.). *The alkaline rocks*, John Wiley and Sons, London, 330-351.
7. **Condie, K.C. (1973).** Archean magmatism and crustal thickening. *Geol. Soc. American Bull.*, v. 84, pp. 2981-2992.
8. **Cox, K.G., Bell, J.D. and Pankhurst, R.J. (1979).** The interpretation of igneous rocks. London. Allen and Unwine, 450 p.
9. **Davies, A., Blackburn, W.H., Brown, W.R. and Ehmann, W.D. (1978).** Trace element geochemistry and origin of Late Precambrian: Early Cambrian Catocin greenstones of the Appalachian Mountains. Univ. of California at Davies, Davies Calif. Rep. (unpublished), cited after Schweitzer J, Kröner A (1985).
10. **El-Gaby, S. (1975).** Petrochemistry and geochemistry of some granites from Egypt. *Neues Jahrbuch Mineralogische Abhandlungen* 124, 147-189.
11. **El Gaby, S., Khudeir, A.A. and El Taky, M. (1989).** The Dokhan Volcanics of Wadi Queih area, central Eastern Desert, Egypt. In: Proceedings of the 1st Conference on Geochemistry, Alexandria University, Egypt, 42–62p.
12. **El Gaby, S., List, F.K. and Tehrani, R. (1990).** The basement complex of the Eastern Desert and Sinai. In: Said, R. (ed.). *The Geology of Egypt*. A.A. Balkema, Rotterdam, Brookfield, 175–199.
13. **El Sheshtawi, Y.A., El Tokhi, M.M. and Ahmed, A.M. (1997).** Petrogenesis of the Dokhan Volcanics of Wadi Dib and Wadi Abu Had, Esh El Mellaha, North Eastern Desert, Egypt. *Ann. Geol. Surv. Egypt* 20, 163–184p.
14. **Ewart, A. (1979).** A review of the mineralogy and chemistry of the Tertiary-Recent dacitic, latitic, rhyolitic and related salic volcanic rocks. In: *Trondhjemites dacites and related rocks* (ed. BARKER, F.) Elsevier, Amsterdam, 13-121.
15. **Ewart, A. (1981).** The mineralogy and petrology of Tertiary-Recent orogenic volcanic rocks: with special reference to the andesitic-basaltic compositional range. In: *Andesites* (ed. THORPE, J.) Elsevier, Amsterdam.
16. **Garson, M.S. and Shalaby, I.M. (1976).** Precambrian-Lower Paleozoic plate tectonics and metallogenesis in the Red Sea Region. *Geol. Assoc. Canada Spec. paper* 14, 573-596p.
17. **Gass, I.G. (1982).** Upper Proterozoic (Pan-African) calc-alkaline magmatism in Northeastern Africa and Arabia. In: R.S. Thorpe (editor), *Andesites and related rocks*. Wiley and Sons, Chichester; New York. 591-609.
18. **Hassan, M.M. (1987).** Abundance and distribution of major elements and their implication on magma type and tectonic setting in the main Proterozoic rock units, Eastern Desert, Egypt. *Int. Symb. Geoch. Prog.* 217, Lund, Sweden.
19. **Heikal, M.A. and Ahmed, A.M. (1984).** Late Precambrian volcanism in Gabal Abu Had, Eastern Desert-Egypt: Evidence for an island-arc environment. *Acta Mineralogica-Petrographica*, Szeged, XXVI/2, 221-233p.

20. **Hermes, O.D., Ballard, R.D. and Banks, P.O. (1978).** Upper Ordovician Peralkaline granites from the Gulf of Maine. *Geol. Soc. Am. Bull.* 80, 1761-1774.
21. **Hildreth, W. (1981).** Gradients in silicic magma chamber: Implications for lithospheric magmatism. *Jour. Geophysical Research*, 86, 10153-10192.
22. **Huang, W.L. and Wyllie, P.J. (1981).** Phase relationships of S-type granite with H₂O to 35kbar: muscovite granite from Harney Peak, South Dakota. *Jour. Geophys. Res.* 86, 10515-10529.
23. **Huppert, H.E. and Sparks, R.S. (1985).** Cooling and contamination of mafic and ultramafic magmas during ascent through continental crust. Elsevier Science Publishers B.V., Amsterdam - Printed in The Netherlands. *Earth and Planeta O' Science Letters*, 74, 371-386p.
24. **Irvine, T.N. and Baragar, W.R.A. (1971).** A guide to the chemical classification of the common volcanic rocks. *Can. Jour. Earth. Sc.* 8, 523-548p.
25. **Le Maitre, R.W. (1976).** The chemical variability of some common igneous rocks. *Jour. Petrology*, 17, 589-637.
26. **Manniar, P.D. and Piccoli, P.M. (1989).** Tectonic discrimination of granitoids. *Geological Society of America Bulletin* 101: 635-643.
27. **McCulloch, M.T. and Gamble, J.A. (1991).** Geochemical and geodynamical constraints on subduction zone magmatism. *Earth. Sci. Lett.* 102, 358-374.
28. **Mohamed, F.H., Moghazi, A.M. and Hassanen, M.A. (2000).** Geochemistry, petrogenesis and tectonic setting of late Neoproterozoic Dokhan-type volcanic rocks in the Fatira area, Eastern- Egypt. *Int. J. Earth Sci.* 88, 764-777p.
29. **Miyashiro, A. (1973).** The Troodos ophiolite complex was probably formed in an island arc. *Earth Planet. Sci. Lett.*, 19, 218-224p.
30. **Miyashiro, A. and Shido, F. (1975).** Tholeiitic and calc-alkalic series in relation to the behaviors of titanium, vanadium, chromium and nickel. *Am. J. Sci.* 275, 265-277p.
31. **Nockolds, S.R. and Allen, R. (1954).** The geochemistry of some igneous rock series: Part II. *Geochim. Cosmochim. Acta* 4, 105-142.
32. **Peacock, M.A. (1931).** Classification of igneous rock series. *J. Geol.* 39, 54-67p.
33. **Pearce, J.A. (1983).** The role of subcontinental lithosphere in magma genesis at destructive plate margins. In: Hawkesworth CJ, Norry HJ (eds) *Continental basalt and mantle xenoliths*. Nantwich, Shiva, 230-249pp.
34. **Pearce, J.A. and Cann, J.R. (1971).** "Ophiolite Origin Investigated by Discriminate Analysis Using Ti, Zr, and Y". *Earth Planet Sci. Lett.* 12:339-349.
35. **Pearce, J.A. and Gale, G.H. (1977).** Identification of ore-deposition environment from trace element geochemistry of associated igneous host rocks. In: *Volcanic Processes in ore Genesis*. Inst. Min. and Metallurgy, Geol. Soc. London, Spec. Publ. 7, 14-24.
36. **Pearce, J.A., Gorman, B.E. and Birkett, T.G. (1977).** The relationship between major element chemistry and tectonic environment of basic and intermediate volcanic rocks. *Earth and Planetary Science Letters*, V. 36, pp. 121-132.
37. **Ragab, A.I. (1987).** On the petrogenesis of the Dokhan volcanics of the northern Eastern Desert of Egypt. *MERC Ain Shams Univ, Earth Sci Ser* 1:151-158p.
38. **Raymond, L.A. (2002).** The study of igneous, sedimentary and metamorphic rocks. McGraw-Hill Higher Education. New York. 128-131.
39. **Ressetar, R. and Monard, J.R. (1983).** Chemical composition and tectonic setting of the Dokhan volcanic formation, Eastern Desert, Egypt. *J Afr Earth Sci* 1: 103-112p.
40. **Ries, A.C., Shackleton, R.M., Graham, R.H. and Fitches, W.R. (1983).** Pan-African structures, ophiolites and mélanges in the Eastern Desert of Egypt. A traverse at 26°N. *J.Geol. Soc. London* 140, 75-95p.
41. **Ringwood, K.E. (1974).** Petrological evolution of the island arc systems. *Jour. Geol. Sec. London*, 130, 183-204.
42. **Rock, N.M.S. (1990).** The International Mineralogical Association (IMA/ CNMMN) pyroxene nomenclature scheme: Computerization and its consequences *Mineralogy and Petrology*, 4 3, 99- 119.
43. **Rollinson, H.R. (1993).** Using geochemical data, evaluation, presentation, interpretation. Longman Group UK Ltd. New York (USA), 197-209p.
44. **Roser, B.P. and Korsch, R.J. (1986).** Determination of tectonic setting of sandstone-mudstone suites using SiO₂ content and K₂O/Na₂O ratio. *Journal of Geology* 94: 635-650.
45. **Saunders, A.D., Tarney, J. and Weaver, S.D. (1980).** Transverse geochemical variations across the Antarctic Peninsula: Implications for the genesis of calc-alkaline magmas. *Earth Planet. Sci. Lett.*, 46, 344-360
46. **Stern, R.J. and Gottfried, D. (1986).** Petrogenesis of late Precambrian (575-600 Ma) bimodal suite in northeast Africa. *Contrib Mineral Petrol* 92: 492-501p.
47. **Strange, P. J., Shaw, R. and Addison, R. (1990).** Geology of Sai Kung and Clear Water Bay. Geotechnical Control Office. Civil Engineering Services Department. HONG KONG. March 1990. Empire Centre, 6th Floor. Tsim Sha Tsui East. Kowloon.
48. **Taylor, S.R. (1965).** Geochemical analyses by spark source mass spectrography. *Geochim. Cosmochim. Acta*, V. 29, pp. 1243-1261.
49. **Taylor, S.R. (1969).** Trace element chemistry of andesites and associated calc-alkaline rocks. In: A.R. McBirney (Editor), *proceedings of the Andesite conference Bull, Oreg.* 372pp.
50. **Thompson, R.N. (1982).** British Tertiary volcanic provenance. *Scott. J. Geol.*, 18, 49-107.
51. **Wilson, M. (2007).** *Igneous Petrogenesis, A global tectonic approach.* Published by Springer, P.O. Box 17, 3300 AA Dordrecht, The Netherlands 4-5p.
52. **Winchester, J.A. and Floyd, P.A. (1977).** Geochemical discrimination of different magma series and their differentiation products using immobile elements. *Chem. Geol.*, V. 20, p. 325-343.
53. **Wood, D.A., Joron, J.L. and Treuil, M. (1979).** "A Re-appraisal of the use of Trace Elements to Classify and Discriminate between Magma Series Erupted in Different Tectonic Settings". *Earth Planet. Sci. Lett.* 45:326-336.